COMPUTER METHODS IN APPLIED MECHANICS AND ENGINEERING 10 (1977) 199–246
© NORTH-HOLLAND PUBLISHING COMPANY

UNIFIED CONCEPTS OF CONSTITUTIVE MODELLING AND NUMERICAL SOLUTION METHODS FOR CONCRETE CREEP PROBLEMS

J.H. ARGYRIS, K.S. PISTER*, J. SZIMMAT and K.J. WILLAM

Institut für Statik und Dynamik der Luft- and Raumfahrtkonstruktionen, University of Stuttgart, 7000 Stuttgart, Germany

Received 15 March 1976

In the first part of the paper an internal variable model is developed for concrete creep with the following features: creep strain is a linear functional of stress history; application or removal of stress produces instantaneous elastic response; upon removal of stress, creep deformations partially recover, approaching in the limit an irrecoverable part. The mechanism of each creep component is affected be temperature, humidity and loading age.

In the second part the internal state variables are derived from concrete creep data with loading ages ranging from 7 to 4560 days and temperatures from 20° to 95°C. Several aging models are examined for which the parameters are determined via least squares optimization. A root mean square criterion is used to assess the approximation.

In the third part a step by step algorithm is developed for incremental solution of the time-dependent creep process, noting that the governing equation of evolution lends itself to an economic computer solution without storing previous results. The one-dimensional constitutive statements are extended to multiaxial conditions and subsequently projected from the local level onto the structural level via finite elements (incremental initial load method).

In the fourth part the creep behaviour of a prestressed concrete reactor vessel is examined for a loading history which includes hygrothermal effects due to drying and heating as well as prestress and cycling pressure.

1. Introduction

There is an extensive body of literature describing experimental results for creep of concrete subjected to prescribed histories of stress. Tests are typically conducted under conditions of uniaxial compression at constant temperature and humidity. Under these conditions, and with the restriction that maximum stress in a given loading program does not exceed approximately 30%–50% of the nominal ultimate strength of the concrete, it appears that a linear, viscoelastic material model adequately predicts creep behaviour. Typical results can be found in work reported in [1–6].

The increasing importance of concrete as a material for reactor containment vessels has necessitated widening the scope of experimental and modelling studies beyond that noted above. In particular there has arisen the need for predicting creep response under non-isothermal conditions, multiaxial stress states and non-uniform moisture content. In addition, the effect of aging in creep response, primarily as a result of the accelerative effect of high temperatures under operating conditions, has become an important factor [7–9].

In the first instance, which we shall refer to as mechanical creep, mathematical structure of the linear viscoelastic model (non-aging) is unambiguous; i.e. such mechanical creep models are always expressible by a hereditary (superposition) integral. However, when aging is considered, this result is largely a matter of formal interest. When one passes to the practical questions of parameterizing

* Department of Civil Engineering, University of California, Berkeley, California 94720, USA.

the kernels of these hereditary integrals (which are the so-called creep functions of the material) and calculating the optimal values of the parameters for best fit of prescribed data, there immediately arise differences of opinion as to what constitutes the "best" parameterization, what experiments should be performed to determine the parameters and what numerical schemes are "best" for calculation. The abundance of published work in this area is adequate testimony to the state-of-the art of these questions and the resulting absence of any consensus among researchers. For representative viewpoints see [10–13].

A much more difficult problem of modelling occurs when concrete is simultaneously subjected to histories of stress, temperature and humidity, especially when aging is of practical importance. To construct models for such conditions on a purely empirical basis is virtually impossible, and even when satisfactory agreement of hypothetical model with a given data set is achieved, its predictive value remains unknown. The difficulty in constructing constitutive models for creep stems from the fact that while creep strain as a good approximation may be assumed to depend linearly on stress history, the dependence on temperature, moisture history and age of loading is very non-linear. Consequently, in addition to the previously described difficulties associated with the definition of mechanical creep functions, one must face the fact that there is no general mathematical structure for thermomechanical creep comparable to that available for linear, isothermal viscoelasticity. Accordingly, the modelling problem must be imbedded as strongly as possible in an appropriate theoretical framework which incorporates at least the following qualities:

(1) adequacy of the constitutive postulates must be supported by qualitative testing with experiments,

(2) structure of the theory should permit a systematic method for improving the flexibility of the model through parameterization,

(3) the resulting constitutive model for creep, when incorporated into a stress analysis program for complex structures, should lend itself to economically feasible computational algorithms.

The objectives of this paper are directly related to these matters. Considerations are limited to plain concrete subjected to prescribed histories of stress, temperature and humidity. We wish to develop a creep model capable of exhibiting the following features:

creep strain is a linear functional of stress history, or in other terms superposition (modified by temperature, humidity and aging) of stress effects is possible; instantaneous application or removal of stress produces corresponding instantaneous (elastic) strain; upon removal of stress, creep recovery ("delayed elasticity") occurs, reaching a limiting value called irrecoverable creep. The mechanisms of each of the above qualitative creep strains will of course be affected by temperature, humidity and aging.

In section 2 we propose as a point of departure a constitutive equation resulting from non-equilibrium thermodynamics based on internal variables. This approach has already been used with some successs to provide the general structure of constitutive equations for viscoelasticity and viscoplasticity. Representative summaries of recent work can be found in [14–17]. First, an internal variable model is developed for non-aging conditions at reference temperature and moisture content based on a first order law of evolution, subsequently extended to account for aging as well as temperature and humidity.

In section 3 the internal variable parameters are identified from concrete creep data with loading ages raging from 7 to 4560 days and temperatures from 20° to 95°C. Several degenerate classes of the unified model are studied introducing different assumptions with regard to aging of the creep components. Least square optimization is applied to obtain the "best" approximation within each

class of aging model. The results are assessed with a root mean square error criterion to quantify the comparison.

In section 4 an incremental algorithm is developed for the numerical solution of complex creep problems with realistic loading histories. To this end, the internal variable model is recast into a recursive algorithm in which history effects of stress, temperature and moisture are fully retained without storing previous results. The local unaxial stress-strain statement is extended to three-dimensional conditions and then projected onto the structural level via finite elements (incremental initial load method). As a result the numerical solution method involves repeated analysis of additional load cases without changing the initial stiffness properties whereby each load case corresponds to advancing the solution by a single time increment.

In section 5 the internal state variable model is applied in the form of finite elements to analyse the long term behaviour of a prestressed concrete reactor vessel. The creep response is examined up to 3 years for a realistic loading history involving hygrothermal effects due to drying and heating as well as mechanical loading due to prestress and cycling pressure with long holding times. This example illustrates the internal variable model for concrete creep when applied to a rather complex engineering problem.

2. Internal variable model for concrete creep

In this section we will present a constitutive equation whose structure is determined from thermodynamics of solids based on internal variables. Inasmuch as our purpose here is one of application and illustration of various approaches to modelling creep, only the necessary results will be stated; the interested reader is referred to works such as [14 and 15] for additional details. For simplicity of presentation the development will be limited to uniaxial (one-dimensional) equations which are generalized in section 4 to multiaxial stress states.

The starting point of our discussion is the concept of thermomechanical state of the material and an associated measure of energy. Here we choose as state variables stress σ, temperature T, humidity H (both relative to an unstressed reference state of the material) and a set of internal variables q_α, where $\alpha = 1, \dots n$. Each of these variables may be a function of time. The internal variables describe internal (microscopic) creep mechanisms and may be related to elements of mechanical models in linear viscoelasticity. However, here they are introduced solely for the purpose of developing a mathematical structure for the creep model and therefore need not have an immediate physical interpretation. We introduce the complementary free energy of the state as

$$\chi = \chi(\sigma, T, H, q_\alpha) . \tag{2.1}$$

It then follows that the constitutive equation for total strain γ at time t can be written

$$\gamma(t) = \frac{\partial \chi}{\partial \sigma} , \tag{2.2}$$

and every creep process must satisfy the dissipation inequality

$$\sum_{\alpha=1}^{n} \frac{\partial \chi}{\partial q_\alpha} \dot{q}_\alpha \geqslant 0 . \tag{2.3}$$

It should be emphasized that these statements are valid for materials in general, irrespective of their constitution, when subjected to mechanical stress, temperature and moisture changes. To define a specific class of materials, one must introduce a constitutive equation for the internal variables which describe the evolution of the inelastic process. Assuming no interaction between individual internal variables, their growth may be characterized by the following state equation

$$\dot{q}_\alpha = f_\alpha(\sigma, T, H, q_\alpha) . \tag{2.4}$$

At this point we must adopt explicit constitutive postulates so that eqs. (2.1), (2.3) and (2.4) acquire mathematical structure. First, (2.3) will be satisfied if we assume

POSTULATE 1

$$\frac{\partial \chi}{\partial q_\alpha} = G_\alpha \dot{q}_\alpha , \tag{2.5}$$

provided that the coefficients G_α are positive. Further, since we are concerned here with a linear theory, we postulate a quadratic form for the complementary energy:

POSTULATE 2

$$X = \frac{1}{2E}\sigma^2 + \tfrac{1}{2}MT^2 + \tfrac{1}{2}NH^2 + \sigma\alpha T + \sigma\beta H + \delta TH + \sum_{\alpha=1}^{n} (A_\alpha q_\alpha \sigma + B_\alpha q_\alpha T + C_\alpha q_\alpha H - \tfrac{1}{2}D_\alpha q_\alpha^2) . \tag{2.6}$$

Substituting this complementary energy expression into (2.2), we obtain the basic creep law

$$\gamma(t) = \underbrace{\frac{\sigma(t)}{E} + \alpha T(t) + \beta H(t)}_{\text{instantaneous}} + \sum_{\alpha=1}^{n} \underbrace{A_\alpha q_\alpha(t)}_{\text{history-dependent}} . \tag{2.7}$$

The total strain γ at time t is composed of instantaneous contributions due to stress, temperature and humidity as well as contributions due to their previous history represented by the internal variables. Substituting the complementary energy expression (2.6) into postulate 1, we obtain the governing equation of evolution for the internal variable $q_\alpha(t)$:

$$G_\alpha \dot{q}_\alpha(t) + D_\alpha q_\alpha(t) = A_\alpha \sigma(t) + B_\alpha T(t) + C_\alpha H(t) . \tag{2.8}$$

This growth equation describes the rate of change of the internal state by a set of first order differential equations with driving forces, stress, temperature and humidity. We observe that postulates 1 and 2 are based on ad hoc constitutive assumptions whose suitability can be examined only in an a posteriori manner, and that the coefficients A_α, B_α, C_α, D_α, G_α, E, M, N, as well as α, β, δ are arbitrary, apart from the restriction that G_α is positive to satisfy eq. (2.3). More general forms, or other mathematical structures, can indeed be employed. We shall now show, however, that those chosen are adequate to describe concrete creep phenomena observed in hygrothermal environments. For algebraic simplicity and clarity we will begin with isothermal, non-aging models at reference humidity.

2.1. The non-aging case at reference temperature and humidity

In this instance A_α, D_α, G_α, E are constants, and with no loss of generality we may assume that $T = T_0 = 0$ and $H = H_0 = 0$ at reference temperature and humidity. Anticipating the need to permit both delayed elasticity and permanent flow in the model, we divide the rate eq. (2.8) into two parts by setting

$$\begin{aligned} \alpha = 1: &\quad D_1 = 0\,, \\ \alpha > 1: &\quad D_\alpha = \text{const.} \end{aligned} \tag{2.9}$$

Solution of the first order differential eq. (2.8) using (2.9) yields for the internal variables

$$\begin{aligned} \alpha = 1: &\quad q_1(t) = \frac{A_1}{G_1} \int_{t_0}^{t} \sigma(\tau)\,\mathrm{d}\tau\,, \\ \alpha > 1: &\quad q_\alpha(t) = \frac{A_\alpha}{G_\alpha} \int_{t_0}^{t} \exp(-\lambda_\alpha(t-\tau))\,\sigma(\tau)\,\mathrm{d}\tau\,, \quad \lambda_\alpha = \frac{D_\alpha}{G_\alpha}\,, \end{aligned} \tag{2.10}$$

where t_0 defines the state of rest for the internal variables. Substituting (2.10) into (2.7) (remembering that $T = 0$ and $H = 0$ at reference temperature and humidity) yields the constitutive equation

$$\gamma(t) = \underbrace{\frac{\sigma(t)}{E}}_{\text{instantaneous}} + \underbrace{\frac{A_1^2}{G_1} \int_{t_0}^{t} \sigma(\tau)\,\mathrm{d}\tau}_{\text{irreversible}} + \underbrace{\sum_{\alpha=2}^{n} \frac{A_\alpha^2}{G_\alpha} \int_{t_0}^{t} \exp(-\lambda_\alpha(t-\tau))\,\sigma(\tau)\,\mathrm{d}\tau}_{\text{delayed}}\,, \tag{2.11}$$

which corresponds to a creep phenomenon comprised of initial elastic response, delayed elastic recovery and permanent flow. This is easily established by recalling that the creep compliance is defined as the total strain at time t produced by a unit stress at time τ. Introducing this condition into eq. (2.11) and integrating yield for the unit creep function

$$\gamma(t)|_{\sigma_\tau = 1} = \mathcal{J}(t-\tau) = \mathcal{J}_0 + \mathcal{J}_1(t-\tau) + \sum_{\alpha=2}^{n} \frac{\mathcal{J}_\alpha}{\lambda_\alpha}\,[1 - \exp(-\lambda_\alpha(t-\tau))]\,, \tag{2.12}$$

where

$$\begin{aligned} &\mathcal{J}_0 = 1/E_0 = \mathcal{J}(0)\,, \\ \alpha = 1: &\quad \mathcal{J}_1 = \frac{A_1^2}{G_1}\,, \\ \alpha > 1: &\quad \mathcal{J}_\alpha = \frac{A_\alpha^2}{G_\alpha}\,, \end{aligned}$$

and λ_α is defined in (2.10). Note that the creep function is parameterized by the constants $\mathcal{J}_0$, $\mathcal{J}_1$, $\mathcal{J}_\alpha$, λ_α, and that the specific creep strain at time t consists of three components for loading at τ:

$$\epsilon_0 = \frac{1}{E_0} = \mathcal{J}(0) = \mathcal{J}_0 \qquad \text{– instantaneous elastic strain,}$$

$$\eta_F = \mathcal{J}_1(t-\tau) \qquad \text{– permanent flow,}$$

$$\eta_D = \sum_{\alpha=2}^{n} \frac{\mathcal{J}_\alpha}{\lambda_\alpha}[1 - \exp(-\lambda_\alpha(t-\tau)) \qquad \text{– delayed elastic strain.}$$

The constitutive eq. (2.11) is readily obtained when the creep function is introduced in the following hereditary creep formula, also known as an impulse formulation:

$$\gamma(t) = \mathcal{J}(0)\sigma(t) - \int_{t_0}^{t} \sigma(\tau)\frac{\partial \mathcal{J}(t-\tau)}{\partial \tau}\,\mathrm{d}\tau\,. \tag{2.13}$$

Alternatively, after integration by parts the step formulation of classical viscoelasticity is recovered:

$$\gamma(t) = \mathcal{J}(t-t_0)\,\sigma(t_0) + \int_{t_0}^{t} \mathcal{J}(t-\tau)\frac{\partial \sigma(\tau)}{\partial \tau}\,\mathrm{d}\tau\,, \tag{2.14}$$

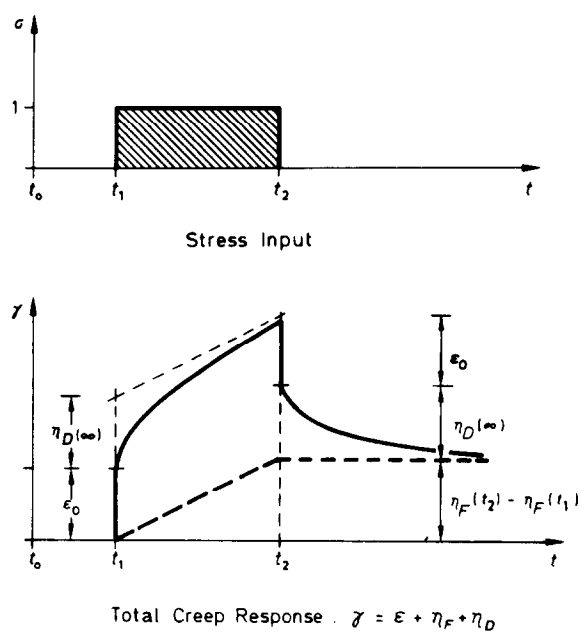

Fig. 1.1. Elastic, flow and delayed elastic deformations, Non-aging creep model.

where $\mathcal{J}(t-\tau)$ denotes the creep strain at time t due to a unit stress applied at time τ.

Fig. 1.1 qualitatively illustrates the strain response associated with the creep function (2.12) resulting from application and removal of a unit stress. The delayed elastic strain asymptotically approaches a limiting value equal to the permanent flow developed at the time of unloading. We note in passing that this creep model is equivalent to a generalized Burgers body consisting of a Maxwell element in series with a chain of Kelvin elements, thus furnishing a mechanical representation of the internal variable formulation.

2.2. The aging case with hygrothermal effects

We have shown that the constitutive postulates (2.5), (2.6), which are built into the mechanical creep model above, lead to qualitatively correct behaviour for concrete. We will now indicate how the model can be generalized to incorporate hygrothermal effects and aging. The rate eq. (2.8) for internal variables controls the evolution of inelastic creep components, i.e. delayed elasticity and flow. Accordingly, we postulate that the coefficients A_α, B_α, C_α, D_α, G_α are all time-dependent, which may result both from hygrothermal environment and aging (maturing); further, in the complementary energy eq. (2.6) we assume that E, α, β are dependent on time, temperature and humidity. To this end the evolution of non-hereditary response components is defined by

$$\begin{aligned} \epsilon(t) &= (1/E)\,[T(t), H(t), t]\;\sigma(t)\,, \\ \eta_T(t) &= \alpha[T(t), H(t), t]\;T(t)\,, \\ \eta_H(t) &= \beta[T(t), H(t), t]\;H(t)\,. \end{aligned} \tag{2.15}$$

In the following we assume that thermal expansion as well as shrinkage or swelling due to moisture transport are predominantly instantaneous. This implies that hereditary components of hygrothermal expansion remain negligible, a hypothesis which appears reasonable in the light of experimental data available at present for concrete [18]. Consequently, temperature and humidity furnish negligible driving forces during the evolution of the creep process, although their effect on material parameters is retained; thus we can assume in (2.8)

$$B_\alpha = C_\alpha = 0\,. \tag{2.16}$$

Analogous to (2.9) we divide the internal variables into flow and delayed components by setting

$$\begin{aligned} \alpha = 1: &\qquad D_1 = 0\,, \\ \alpha > 1: &\qquad D_\alpha = D_\alpha(t)\,. \end{aligned} \tag{2.17}$$

With these assumptions eq. (2.8) is readily solved for the internal variables in the form of an integral expression similar to (2.10):

$$\alpha = 1: \quad q_1(t) = \int_{t_0}^{t} \frac{A_1(\tau)}{G_1(\tau)} \sigma(\tau)\, \mathrm{d}\tau ,$$

$$\alpha > 1: \quad q_\alpha(t) = \int_{t_0}^{t} \frac{A_\alpha(\tau)}{G_\alpha(\tau)} \exp[-\xi_\alpha(t) + \xi_\alpha(\tau)]\ \sigma(\tau)\, \mathrm{d}\tau , \tag{2.18}$$

where the exponent of the delayed contribution is in itself an integral expression transforming real time into "effective" time ξ:

$$\xi_\alpha(t) = \int_{t_0}^{t} \frac{D_\alpha(s)}{G_\alpha(s)} \mathrm{d}s , \quad \xi_\alpha(\tau) = \int_{t_0}^{t} \frac{D_\alpha(s)}{G_\alpha(s)} \mathrm{d}s . \tag{2.19}$$

Substituting (2.18) and (2.19) into eq. (2.7) gives the creep equation for hygrothermal environments:

$$\gamma(t) = \epsilon(t) + \eta_T(t) + \eta_H(t) + A_1(t) \int_{t_0}^{t} \frac{A_1(\tau)}{G_1(\tau)} \sigma(\tau)\, \mathrm{d}\tau$$

$$+ \sum_{\alpha=2}^{n} A_\alpha(t) \int_{t_0}^{t} \frac{A_\alpha(\tau)}{G_\alpha(\tau)} \exp[-\xi_\alpha(t) + \xi_\alpha(\tau)]\ \sigma(\tau)\, \mathrm{d}\tau . \tag{2.20}$$

To proceed further with this generalization of (2.11), it is evident that additional constitutive assumptions are required. Before examining five important classes of aging, we recall the structure of the growth law (2.8). Obviously, there is no loss of generality if we assume that A_1 and A_α are constants in order to normalize the rate equation; thus (2.20) can be rewritten

$$\gamma(t) = \epsilon(t) + \eta_T(t) + \eta_H(t) + \eta_q(t) . \tag{2.21}$$

The instantaneous components ϵ, η_T, η_H are specified by eq. (2.15), while the hereditary contribution η_q is composed of aging flow and aging delayed components

$$\eta_q(t) = \eta_F(t) + \eta_D(t) , \tag{2.22}$$

with

$$\eta_F(t) = A_1^2 \int_{t_0}^{t} \frac{1}{G_1(\tau)} \sigma(\tau)\, \mathrm{d}\tau ,$$

$$\eta_D(t) = \sum_{\alpha=2}^{n} A_\alpha^2 \int_{t_0}^{t} \frac{1}{G_\alpha(\tau)} \exp[-\xi_\alpha(t) + \xi_\alpha(\tau)]\ \sigma(\tau)\, \mathrm{d}\tau . \tag{2.23}$$

2.3. Special classes of aging

Let us now examine several classes of aging by introducing more specific constitutive structure into flow and delayed elastic components, omitting for the time being the instantaneous components.

Case 1. Aging flow model $\eta_q = \eta_F(t)$ (2.24)

In this case we assume that there is no delayed action, i.e. $\alpha < 2$ with $\eta_D(t) = 0$; thus hereditary creep is described by an aging flow mechanism in terms of a *single* function of time τ, i.e. the age or rather the maturity of the concrete at loading. Let us introduce the hygrothermal aging function Ψ by setting

$$\frac{1}{G_1(\tau)} = \Psi[T(\tau), H(\tau), \tau] \; ; \tag{2.25}$$

then $\Psi(\tau)$ defines the rate of flow produced by a unit stress input at time τ. Integration over the entire life span $t_0 - t$ yields for the irreversible flow component

$$\eta_F(t) = A_1^2 \int_{t_0}^{t} \Psi[T(\tau), H(\tau), \tau] \; \sigma(\tau)\, \mathrm{d}\tau \, . \tag{2.26}$$

For a unit stress from $t_1 - t$ the specific flow is given by integration of the flow rate (2.25):

$$\eta_F(t)|_{\sigma=1} = g(t) - g(t_1) \, ,$$

where

$$g(t) = \int_{t_0}^{t} \Psi[T(\tau), H(\tau), \tau] \; \mathrm{d}\tau \tag{2.27}$$

and

$$g(t_1) = \int_{t_0}^{t_1} \Psi[T(\tau), H(\tau), \tau] \; \mathrm{d}\tau$$

define the unit creep function, i.e. the creep strain for unit loading. For time variable stresses superposition is defined by (2.26) corresponding to the convolution integral expression (2.13). This formulation is essentially the time-hardening method known in concrete literature also as the "Rate of Creep" method [3, 19]. Rheologically speaking, the model is equivalent to an aging Maxwell unit.

Case 2. Delayed elastic model $\eta_q = \eta_D(t - \tau)$ (2.28)

In this case we assume that there is no flow and that the hereditary contribution is described by a non-aging delayed component in terms of a single function of time elapsed since loading $t - \tau$.

In correspondence with (2.10) we set

$$\alpha > 1: \quad G_\alpha(\tau) = \text{const} \quad \text{and} \quad D_\alpha(\tau) = \text{const} \tag{2.29}$$

so that $\lambda_\alpha = D_\alpha / G_\alpha$ reduces the equivalent time scale, eq. (2.19), back into a linear function of real time

$$\xi_\alpha(t) = \lambda_\alpha(t - t_0) \quad \text{and} \quad \xi_\alpha(\tau) = \lambda_\alpha(\tau - t_0)\,. \tag{2.30}$$

In this case the delayed elastic creep component is described by an exponential series in terms of load duration $t - \tau$ as an independent variable:

$$\eta_D(t - t_0) = \sum_{\alpha=2}^{n} \mathcal{J}_\alpha \int_{t_0}^{t} \exp(-\lambda_\alpha(t - \tau))\ \sigma(\tau)\,\mathrm{d}\tau\,, \qquad \mathcal{J}_\alpha = \frac{A_\alpha^2}{G_\alpha}\,. \tag{2.31}$$

For a unit stress $\sigma = 1$ in the interval t_1 to t the specific delayed component is readily obtained by integration:

$$\eta_D(t - t_1)|_{\sigma=1} = \sum_{\alpha=2}^{n} \frac{\mathcal{J}_\alpha}{\lambda_\alpha}\,[1 - \exp(-\lambda_\alpha(t - t_1))]\,, \tag{2.32}$$

which defines the unit creep function, i.e. the creep strain for unit loading. For variable stress histories, superposition is specified by a convolution integral which corresponds to the impulse formulation (2.13). Rheologically speaking, this model corresponds to a chain of non-aging Kelvin solids.

Case 3. Summation model $\eta_q(t) = \eta_F(t) + \eta_D(t - \tau)$ (2.33)

In this case we assume that hereditary creep is composed of aging flow as well as a non-aging delayed elastic contribution. In contrast to the previous two cases, creep is now described by two independent functions. Adding the two components (2.26) and (2.31), we obtain

$$\eta_q(t) = A_1^2 \int_{t_0}^{t} \Psi[T(\tau), H(\tau), \tau]\ \sigma(\tau)\,\mathrm{d}\tau + \sum_{\alpha=2}^{n} \mathcal{J}_\alpha \int_{t_0}^{t} \exp(-\lambda_\alpha(t - \tau))\ \sigma(\tau)\,\mathrm{d}\tau\,. \tag{2.34}$$

For unit stress input $\sigma = 1$ applied at different loading ages between t_0 and t this creep model spans a surface in the two independent variables, age t and load duration $t - t_i$; then

$$\eta_q(t)|_{\sigma=1} = g(t) - g(t_i) = \sum_{\alpha=2}^{n} \frac{\mathcal{J}_\alpha}{\lambda_\alpha}\,[1 - \exp(-\lambda_\alpha(t - t_i))]\,. \tag{2.35}$$

For variable stress histories, superposition is defined by a convolution integral expression corresponding to the impulse formulation (2.13). The resulting creep model is essentially the "rate of flow" method described in [12, 20]. Rheologically speaking, it corresponds to a generalized Burgers body with an aging Maxwell unit.

Case 4. Product model $\eta_q(t) = \eta_D(\tau, t-\tau)$ (2.36)

In this case we assume that the flow component is zero, $\eta_F(t) = 0$, and that hereditary creep is expressed by an delayed mechanism in which aging is introduced in the form of a product of two functions – one defines the age, i.e. the maturity of the concrete, and the other the creep rate since loading. To this end we assume that aging is reflected by the coefficients G_α and D_α in such a way that they are fully described by a single aging function Φ:

$$\alpha > 1: \quad \frac{1}{G_\alpha(\tau)} = \Phi[T(\tau), H(\tau), \tau] \ , \qquad D_\alpha(\tau) = \lambda_\alpha / \Phi[T(\tau), H(\tau), \tau] \ . \tag{2.37}$$

The transformation of time scale in this case is linear since

$$\frac{D_\alpha(\tau)}{G_\alpha(\tau)} = \lambda_\alpha = \text{const},$$

and thus

$$\xi_\alpha(t) = \lambda_\alpha(t - t_0) \quad \text{and} \quad \xi_\alpha(\tau) = \lambda_\alpha(\tau - t_0) \ . \tag{2.38}$$

Introducing these constitutive assumptions into (2.23) leads to the following expression for the delayed elastic component:

$$\eta_D(\tau, t-\tau) = \sum_{\alpha=2}^{n} A_\alpha^2 \int_{t_0}^{t} \Phi[T(\tau), H(\tau), \tau] \exp(-\lambda_\alpha(t-\tau))\, \sigma(\tau)\, \mathrm{d}\tau \ . \tag{2.39}$$

Formally, (2.39) defines a rule of superposition of strains which is more general than the classical convolution integral equation. The aging function Φ weights the delayed elastic action in the form of a homothetic product law. This affine transformation model corresponds to the classical creep formulations for aging concrete [1, 2, 4, 21], the only difference being that here the impulse formulation is used instead of the step formulation (see (2.13) versus (2.14)).

Case 5. Effective time model $\eta_q(t) = \eta_D(\xi_t - \xi_\tau)$ (2.40)

In this case we assume that aging and hygrothermal effects are reflected *only* by G_α in the rate eq. (2.8), with the further provision that all coefficients are *equal*. Thus $\alpha > 1$

$$\alpha > 1: \quad \frac{1}{G_\alpha(\tau)} = \Phi[T(\tau), H(\tau), \tau] \ , \qquad D_\alpha(\tau) = \text{const} \ . \tag{2.41}$$

Recalling the transformation of real time into effective time in eq. (2.19), we obtain

$$\xi_\alpha(t) = D_\alpha \xi_t \quad \text{and} \quad \xi_\alpha(\tau) = D_\alpha \xi_\tau ,$$

$$\text{with} \quad \xi_t = \int_{t_0}^{t} \Phi[T(s), H(s), s] \, \mathrm{d}s \quad \text{and} \quad \xi_\tau = \int_{t_0}^{\tau} \Phi[T(s), H(s), s] \, \mathrm{d}s . \tag{2.42}$$

Considering that

$$\mathrm{d}\xi_\tau = \frac{1}{G_\alpha(\tau)} \, \mathrm{d}\tau = \Phi[T(\tau), H(\tau), \tau] \, \mathrm{d}\tau , \tag{2.43}$$

we can change the variables of integration in (2.23) and obtain

$$\eta_D(\xi_t - \xi_0) = \sum_{\alpha=2}^{n} A_\alpha^2 \int_{\xi_0}^{\xi_t} \exp(-D_\alpha(\xi_t - \xi_\tau)) \, \sigma(\xi_\tau) \, \mathrm{d}\xi_\tau , \tag{2.44}$$

which defines creep in the form of a delayed elastic model in the effective time ξ to account for aging as well as hygrothermal effects. For a unit stress input $\sigma = 1$ in the interval $t_1 - t$ the unit creep function is obtained by integration:

$$\eta_D(\xi_t - \xi_1)|_{\sigma=1} = \sum_{\alpha=2}^{n} (A_\alpha^2/D_\alpha) \, [1 - \exp(-D_\alpha(\xi_t - \xi_1))] . \tag{2.45}$$

For time-variable stresses the superposition is specified by a convolution integral corresponding to the impulse formulation (2.13). The resulting effective time model corresponds to the time shift hypothesis of thermorhelogically simple materials and was applied to concrete for environmental effects in [7] and aging in [22, 23]. In the last two references the step formulation was used instead of the impulse formulation.

3. Identification of internal variables

In this section recent creep data from a long term testing program [24] are used to identify the internal state variable parameters. Inasmuch as our purpose here is to illustrate the identification procedure and to assess the accuracy of the proposed creep formulation, we will concentrate on the problem of "best approximation" of creep considering aging in the range from 7 to 4560 days at two temperatures, $T = 20°C$ and $T = 95°C$. We note that testing was confind to isothermal conditions; thus extension to temperature transients would require further elaboration on possible transitional thermal effects [8, 26]. Moreover, the experimental program was carried out on fully saturated specimens; thus additional test data are required to account for different humidity conditions or drying creep.

3.1. Concrete creep data

As a starting point for our discussion we will briefly review creep data presented recently for the Wylfa reactor concrete [24] for which an extensive test program has been carried out at Taylor Woodrow for the last 12.5 years [25].

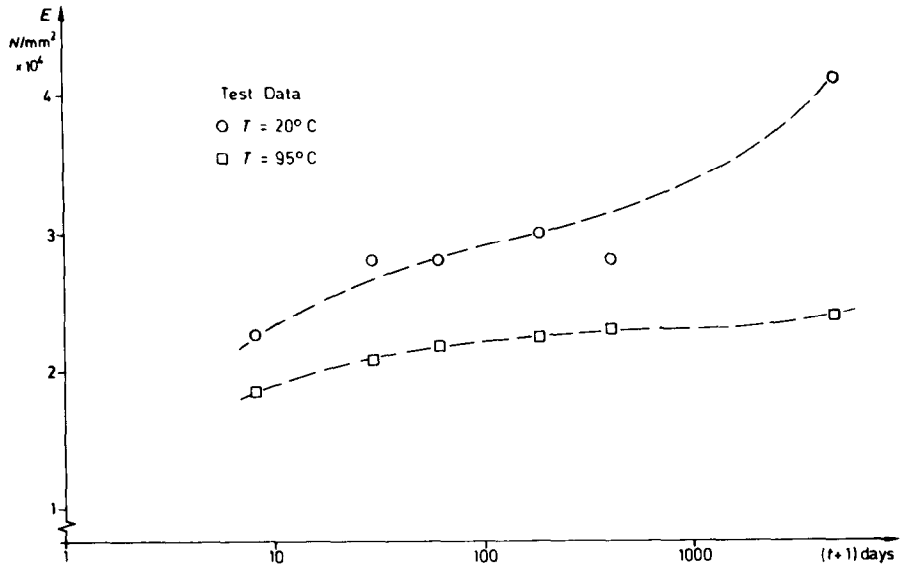

Fig. 3.1. Aging elastic behaviour, Wylfa concrete data (Browne and Bamforth).

Fig. 3.1 shows the effect of age on the modulus of elasticity. It indicates that the concrete matures considerably at room temperature; during 12.5 years of observation the modulus of

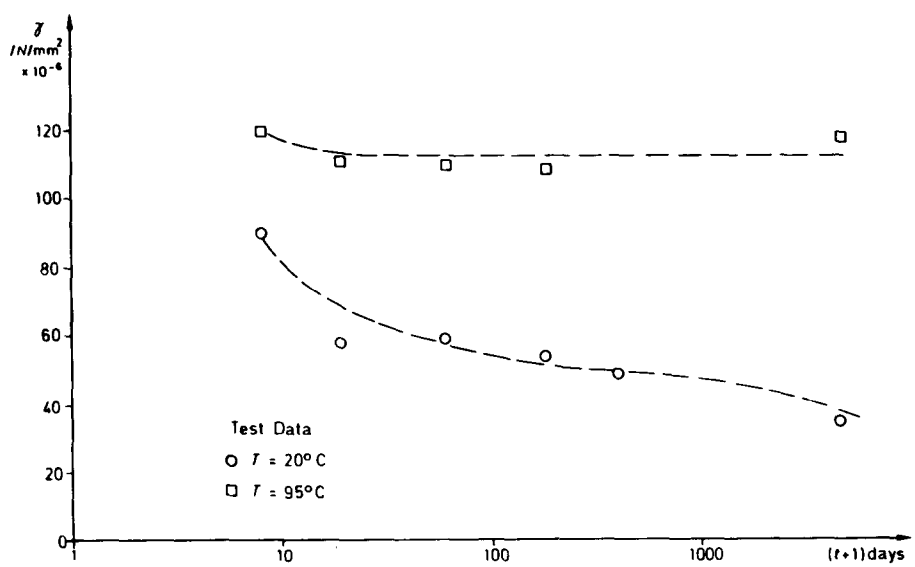

Fig. 3.2. Creep deformations after loading for 102 days, Wylfa concrete data (Browne and Bamforth).

elasticity increase by 82%. In contrast, at 95°C there is very little aging of the instantaneous response.

Fig. 3.2 shows the effect of age on total deformations when the specimens are loaded for 102 days. It indicates again that concrete matures considerably at room temperature; during 12.5 years of observation the creep response reduces by 61%. In contrast, at $T = 95$°C there is virtually no aging effect on total strains.

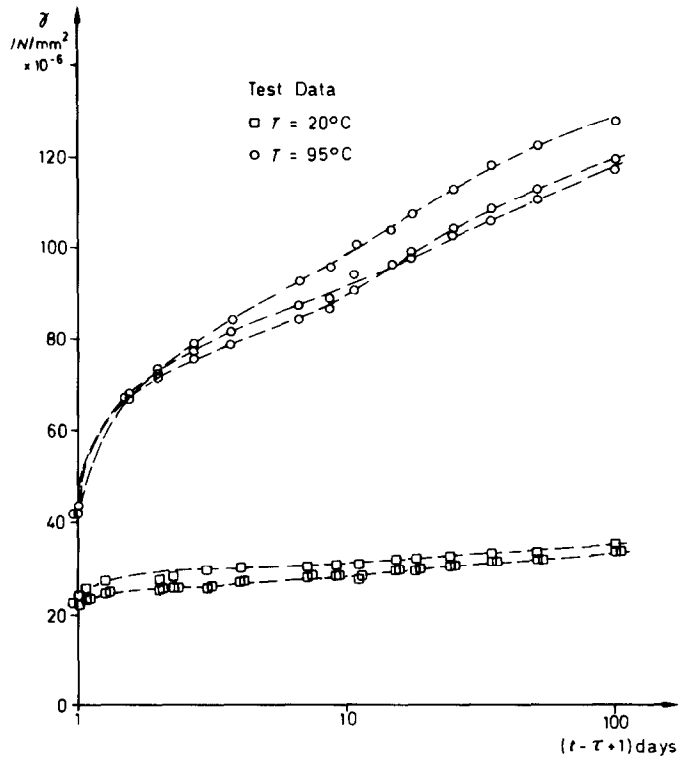

Fig. 3.3. Creep deformations for loading at 2.5 years, Wylfa concrete data (Browne and Bamforth).

For completeness, a thrid result is taken from [24] to illustrate the time variation of creep when loaded at 12.5 years. Fig. 3.3 shows the undiminished creep capacity at 95°C as opposed to the reduced response at room temperature. In this context we note the scatter of experimental data which amounts to approximately 5 microstrain per N/mm^2 at 20°C and 10 microstrain per N/mm^2 at 95°C (1 microstrain = 10^{-6} mm/mm).

For subsequent parameter identification these test data are utilized together with previous results reported in [25] to construct a set of creep curves for four loading ages, 7, 28, 400 and 4560 days, and two temperatures, 20°C and 95°C. As a first step, we consider the effect of aging at reference temperature $T = T_0 = 20$°C. From the physics of the creep process we postulate that the total creep strain must be a monotonically increasing function of load duration $t - \tau$; thus

$$\frac{\partial}{\partial(t-\tau)}\,[\gamma(t-\tau,\tau)] \geqslant 0\,, \tag{3.1}$$

whereby the creep rate decreases at least during primary creep. Moreover, from the process of chemical maturing we postulate that the total creep strain must be a monotonically decreasing

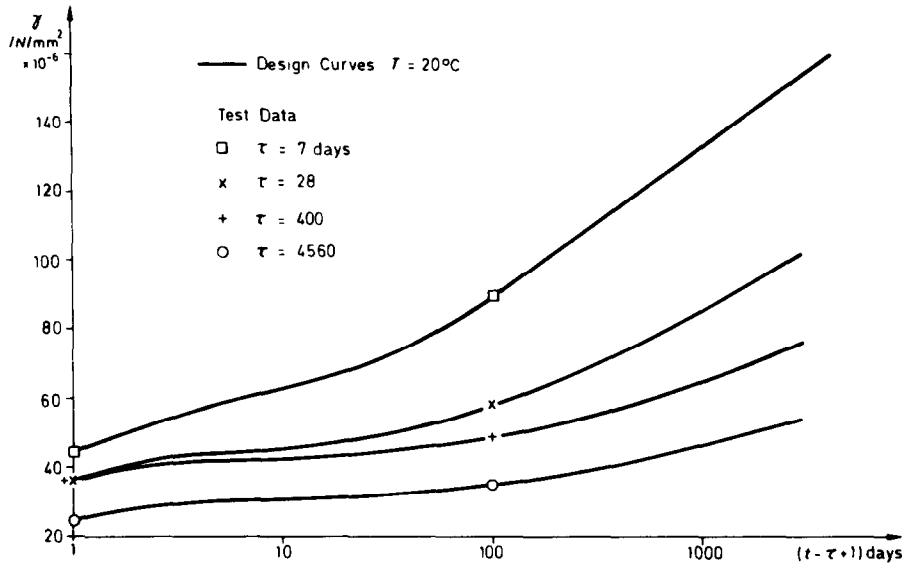

Fig. 3.4. Design curves for aging creep at $T = 20°C$, Wylfa concrete data (Browne and Bamforth).

function of loading age τ, thus

$$\frac{\partial}{\partial \tau}[\gamma(t-\tau,\tau)] \leqslant 0\,. \tag{3.2}$$

With these observations in mind we can now design a set of creep curves from the data shown in figs. 3.2, 3.3. The results are indicated in fig. 3.4 for a load duration $t - \tau$ from 0 up to 3000 days and for four loading ages $\tau = 7$, 28, 400 and 4560 days. The creep curves pass through the corresponding data points of instantaneous elastic response $t - \tau = 0$ and creep response after loading for $t - \tau = 102$ days. Since there is virtually no aging of the elastic component for loading between 28 and 400 days, the associated creep curves start at the same origin.

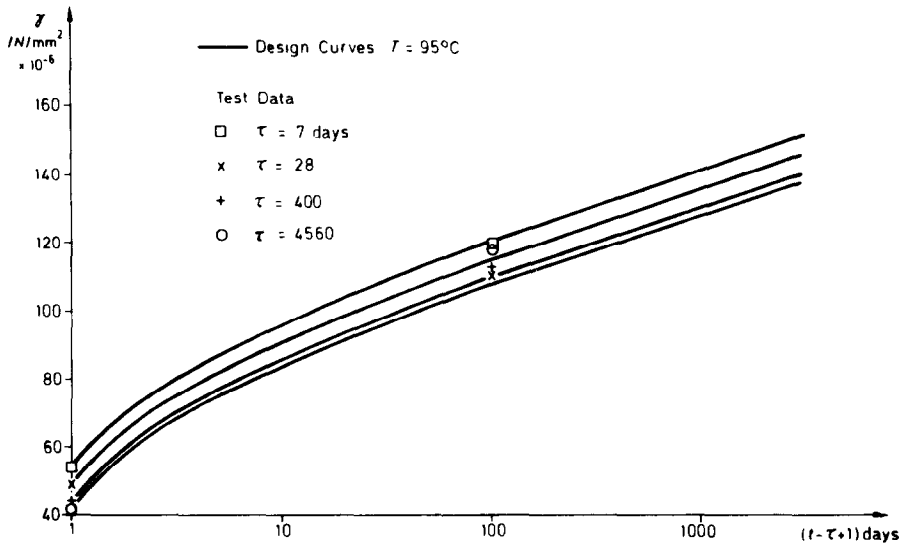

Fig. 3.5. Design curves for aging creep at $T = 95°C$, Wylfa concrete data (Brown and Bamforth).

As a second step, we examine now the effect of temperature considering the total deformations from creep tests at $T = 95°C$. Fig. 3.5 shows the experimental data, i.e. the instantaneous elastic strains at loading ages 7, 28, 400 and 4560 days, and the creep deformations after load duration $t - \tau = 102$ days. Conversely to the case with $T = 20°C$ there is very little aging because of cyclic heat treatment before loading. As a matter of fact, some of the test data violate condition (3.2). Since the scatter all lies within the experimental error, it is reasonable to assume that aging is confined to the instantaneous elastic response. Therefore, the creep curves for different loading ages are obtained from a single master curve by vertical translation as shown in fig. 3.5.

3.2. Least squares identification

For a valid comparison of different classes of aging, an unbiased procedure is needed to assign the "best" parameter values to each model. To this end an *objective* identification technique has to be developed using a method such as least squares optimization, which minimizes the error between input data y_j and their approximations $f(x_j)$ with internal variable models at $j = 1, 2, \ldots M$ sampling points [27]. The optimization problem is then posed as

$$\Delta = \sum_{j=1}^{M} [f(x_j) - y_j]^2 \rightarrow \text{Min.} \tag{3.3}$$

The resulting root mean square error provides an objective measure for the average deviation at each data point. Normalization by the input data y_j yields the following relative error:

$$\delta_M = \Delta_M / Y_M \quad \text{with} \quad \Delta_M = (\Delta/M)^{1/2} \text{ and RMS average: } Y_M = \left[\sum_{j=1}^{N} (y_j)^2 / M\right]^{1/2}, \tag{3.4}$$

which is used below to quantify the accuracy for different classes of aging.

A modified Marquardt algorithm is used for finding the minimum of the sum of squares of M functions. This algorithm is a combination of Newton's method and steepest descent optimization and is available in most software libraries. In our particular case the CDC–IMSL library package is used. Note that the Marquardt algorithm has been applied previously [28] for the identification of two-dimensional creep surfaces, without assigning definite structure to the unit creep function.

We proceed now with a simple example to illustrate the identification via least squares optimization. To this end we consider the one-dimensional curve fitting problem for the instantaneous elastic response as a function of age. Clearly, from the process of chemical mataring we can conclude that the elastic strain must be a monotonically decreasing function to time, thus

$$\dot{\epsilon}(t) = \frac{\partial}{\partial t}\left[\frac{1}{E(t)}\right] \leqslant 0 . \tag{3.5}$$

Let us first consider an approximation by exponential series expansion for unit stress:

$$\epsilon(t)|_{\sigma=1} = \sum_{i=1}^{N} a_i \exp(-c_i t) , \tag{3.6}$$

which satisfies condition (3.5) for positive a_i and c_i. We recall [29] that there is no unique solution for a_i, c_i, and that we obtain numerically equivalent approximations if we assign fixed values to the exponents c_i, i.e. the relaxation spectrum of interest. In this way, the number of unknown parameters is reduced to the number of terms in the exponential series N, which in our case is also an optimization variable. Experimental studies have shown that relaxation times must be well separated; thus different decades are assigned to the exponents c_i:

$$\begin{aligned} i = 1: &\quad c_1 = 0\,, \\ i > 1: &\quad c_i = 3 \times 10^{-(i-1)}\,. \end{aligned} \tag{3.7}$$

Considering the test data indicated in fig. 3.1, we have in this case 6 sampling points $j = 1, 2, \ldots M = 6$, at which

$$y_j = \frac{1}{E(t_j)} \quad \text{with RMS average: } Y_M^\epsilon = 35.33 \times 10^{-6} \text{ per N/mm}^2\,. \tag{3.8}$$

At times t_j the exponential approximation is readily obtained from (3.6):

$$f(x_j) = \epsilon(t_j) = \sum_{i=1}^{N} a_i \exp(-c_i t_j)\,. \tag{3.9}$$

Marquardt least squares optimization yields in this case a global optimum for an exponential series with $N = 6$. The parameters are

i	c_i	a_i ($T = 20°$)	a_i ($T = 95°$)	
1	0	0.113	31.281	
2	0.3	64.791	0	
3	0.03	0.819	11.099	$N = 6$
4	0.003	0	1.092	$M = 6$
5	0.0003	10.766	0.079	
6	0.00003	25.248	11.977	
$\delta_M = \Delta_M / Y_M^\epsilon$		0.028	0.009	

(3.10)

The resulting aging functions $\epsilon(t)$ are shown in fig. 3.6 and indicate a rather close fit even for the unsmoothed data with $\epsilon(400) > \epsilon(180)$ at $T = 20°$C.

In what follows, the Marquardt least squares optimization is applied to the identification of aging creep within the frame of non-aging as well as aging models. Geometrically speaking, we are confronted with the approximation of a creep surface as a function of loading age τ and load duration $t - \tau$, as shown in fig. 3.4, where the total deformation is in general made up of several time-dependent components.

3.3. Non-aging models

As a first step we consider the case of non-aging behaviour for which the problem reduces to the identification of the constant coefficients $\mathcal{J}_0, \mathcal{J}_1$ and $\mathcal{J}_\alpha$ in eq. (2.12). For least squares opti-

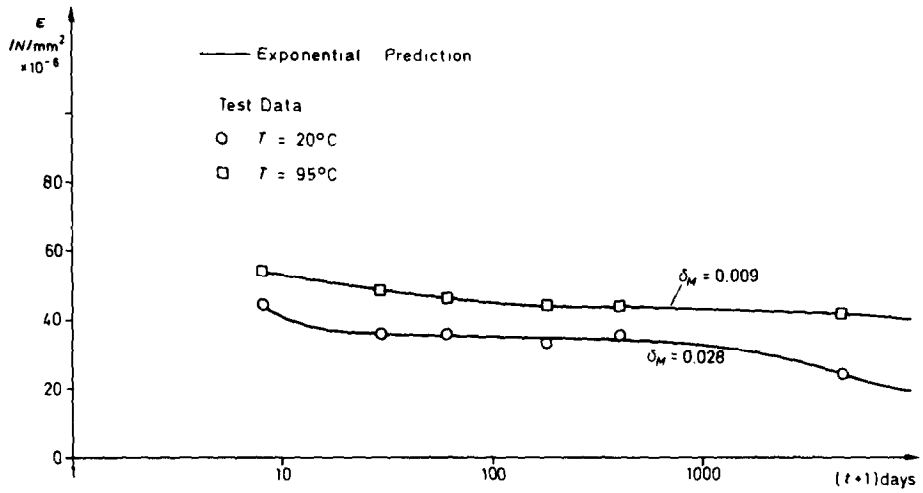

Fig. 3.6. Exponential approximation of elastic compliance, Wyfla concrete data (Brown and Bamforth).

mization we extract from fig. 3.4 a set of data points by dividing the time under loading $t - \tau =$ 3000 days into 14 intervals which are equally spaced on a logarithmic scale. For the four loading ages $\tau = 7, 28, 400$ and 4560 days this yields data values at the sampling points

$$y_j = \gamma(t_k - \tau_l, \tau_l) \quad \text{with RMS average: } Y_M^\gamma = 67.69 \times 10^{-6} \text{ per N/mm}^2 , \tag{3.11}$$

where

$$k = 1, 2, \ldots 14 ; \quad l = 1, 2, \ldots 4 ; \quad M = 14 \times 4 = 56 . \tag{3.12}$$

Now we apply the identification procedure to three classical cases of linear viscoelasticity: the Maxwell unit, the Kelvin chain and the generalized Burgers model.

Maxwell unit: $\gamma(t) = \epsilon_0 + \eta_F(t)$ (3.13)

In this case the creep surface is approximated by a linear function of time t:

$$\gamma(t)|_{\sigma=1} = \vartheta_0 + \vartheta_1 t - \vartheta_1 \tau , \tag{3.14}$$

which has to be evaluated at the sampling points in terms of the optimization variables ϑ_0, ϑ_1:

$$f(x_j) = \vartheta_0 + \vartheta_1(t_k - t_l) , \quad k = 1, 2, \ldots 14 ; \quad l = 1, 2, \ldots 4 . \tag{3.15}$$

The best approximation is readily identified with the Marquardt least squares procedure yielding a relative RMS error of

$$\delta_M = 0.359 .$$

The optimum parameter values are

$$\mathcal{J}_0 = \frac{1}{E_0} = 51.7\,, \quad \mathcal{J}_1 = 0.019\,, \quad N = 2\,, \quad M = 56\,. \tag{3.16}$$

Kelvin chain: $\gamma(t) = \epsilon_0 + \eta_D(t - \tau)$ (3.17)

In this case the creep surface is approximated by an exponential series in the independent variable $t - \tau$:

$$\gamma(t-\tau)|_{\sigma=1} = \mathcal{J}_0 + \sum_{\alpha=2}^{n} \frac{\mathcal{J}_\alpha}{\lambda_\alpha}[1 - \exp(-\lambda_\alpha(t_k - t_l))]\,, \quad \mathcal{J}_\alpha = \frac{A_\alpha^2}{G_\alpha}\,, \tag{3.18}$$

which has to be evaluated at the sampling points in terms of $N = n$ optimization variables $\mathcal{J}_0$, $\mathcal{J}_\alpha$:

$$f(x_j) = \mathcal{J}_0 + \sum_{\alpha=2}^{n} \frac{\mathcal{J}_\alpha}{\lambda_\alpha}[1 - \exp(-\lambda_\alpha(t_k - t_l))]\,, \quad k = 1, 2, \ldots 14\,; \quad l = 1, 2, \ldots 4\,. \tag{3.19}$$

The optimum parameter values are readily identified with the Marquardt least squares procedure for a variable number of terms in the exponential series ($n = 2, \ldots 8$). The best approximation is obtained for $n = 6$ with a relative RMS error of

$$\delta_M = 0.335\,.$$

The corresponding parameters are

$$\mathcal{J}_0 = \frac{1}{E_0} = 37.0 \tag{3.20}$$

and

i	λ_α	$\mathcal{J}_\alpha$	
1	3.0	3.28	
2	0.3	1.71	
3	0.03	0.205	
4	0.003	0.073	$N = 6$
5	0.0003	0.011	$M = 6$

(3.21)

Generalized Burgers body: $\gamma(t) = \epsilon_0 + \eta_F(t) + \eta_D(t - \tau)$ (3.22)

In this case the creep surface is approximated by the sum of a linear function of time t and an exponential expansion in $t - \tau$:

$$\gamma(t-\tau)|_{\sigma=1} = \mathcal{J}_0 + \mathcal{J}_1(1 - \tau) + \sum_{\alpha=2}^{n} \frac{\mathcal{J}_\alpha}{\lambda_\alpha}[1 - \exp(-\lambda_\alpha(t - \tau))]\,, \tag{3.23}$$

which has to be evaluated at M sampling points in terms of $N = n + 1$ optimization variables $\mathcal{J}_0$, $\mathcal{J}_1$, $\mathcal{J}_\alpha$:

$$f(x_j) = \mathcal{J}_0 + \mathcal{J}_1 (t_k - t_l) + \sum_{\alpha=2}^{n} \frac{\mathcal{J}_\alpha}{\lambda_\alpha} [1 - \exp(-\lambda_\alpha (t_j - t_k))] \ , \quad k = 1, 2, \ldots 14; \quad l = 1, 2, 3, 4 \ , \tag{3.24}$$

Again, the optimum parameter values are readily identified with the Marquardt least squares procedure for a variable number of terms in the exponential series ($n = 2, \ldots 8$). The best approximation is obtained for $n = 5$ with a root mean square error of

$$\delta_M = 0.335.$$

The corresponding parameters are

$$\mathcal{J}_0 = \epsilon_0 = \frac{1}{E_0} = 36.9 \ , \qquad \mathcal{J}_1 = 0.0064 \ , \tag{3.25}$$

and

i	λ_α	$\mathcal{J}_\alpha$	
1	3.0	3.28	
2	0.3	1.84	$N = 6$
3	0.03	0.172	$M = 56$
4	0.003	0.085	

(3.26)

Fig. 3.7 shows creep predictions which result from the three non-aging creep models. For comparison, the original design curves are included for four loading ages indicating considerable deviation because of aging. The figure also shows that the Kelvin chain and Burgers model are virtually identical since the flow term $\mathcal{J}_1$ almost vanishes (see eq. (3.26)). Therefore, we can conclude that linear flow

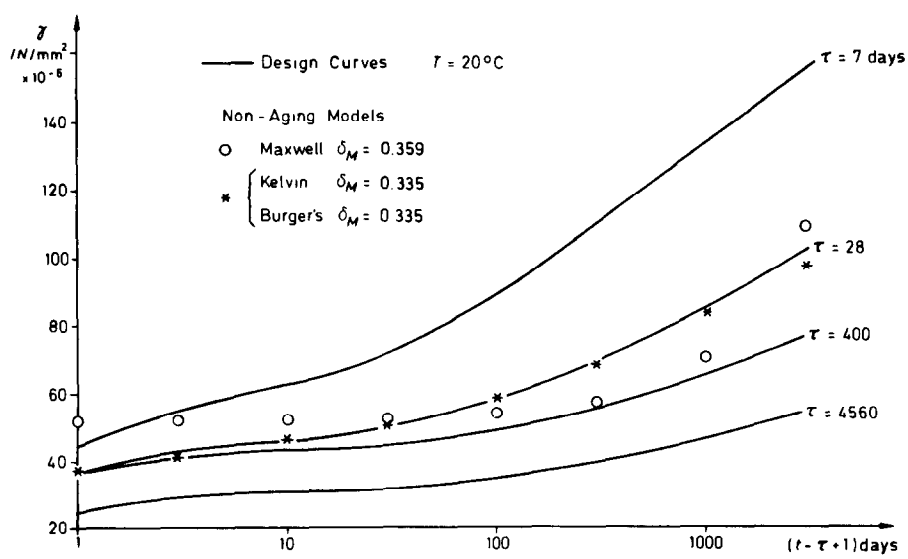

Fig. 3.7. Approximation of creep surface with non-aging viscoelastic models.

is reproduced by exponential expansion and could be omitted if a sufficiently large number of exponentials were used. On the other hand, if only a small number of terms are used, then linear flow considerably improves the total approximation. Moreover, the comparison is confined here to creep under constant load, If we consider unloading, then we recall that the Kelvin chain predicts complete creep recovery while the flow component in Burgers model introduces an irreversible contribution. It has been observed [5] that concrete exhibits only very limited recovery when unloaded; thus, for application to loading as well as unloading regimes, creep recovery should also be considered for identification. In this light the Maxwell unit without recovery and the Kelvin chain with full recovery are at disadvantage when compared with Burgers model in which only a *limited* retardation spectrum is used for the delayed component.

3.4. Aging models

In section 2.3 five classes of aging were developed from the general internal variable model making different assumptions for $G_\alpha(t)$, $D_\alpha(t)$ in the equation of evolution (2.8). In the following, parameters in these various cases are identified with the Marquardt least squares procedure. Inasmuch as these aging models are concerned exclusively with the hereditary component η_q, we redefine our design curves by substracting the instantaneous elastic components. With $T_0 = 0$ and $H_0 = 0$,

$$\eta_q(t) = \gamma(t) - \epsilon(t) . \tag{3.27}$$

The time variation is obtained by shifting the creep curves in fig. 3.4 vertically to the origin. The resulting design curves are used as input values for the identification below:

$$y_j = \gamma(t_k - t_l, t_l) - \epsilon(t_l) \quad \text{with RMS average: } Y_M^\eta = 36.16 \times 10^{-6} \text{ per N/mm}^2 , \tag{3.28}$$

where

$$j = 1, 2, \ldots M = 56 \quad \text{and} \quad k = 1, 2, \ldots 14 ; \quad l = 1, 2, 3, 4 .$$

In proceeding to the different classes of aging models we observe that the algebraic identification problem for the non-aging models is now complicated by the fact that *functions* have to be identified. In the case of aging flow and delayed elastic formulations the creep surface is described by a *single* function, while for the summation and the product model as well as in the time shift model *two* functions are used. Clearly, these functions have to be parametrized before least squares identification; to this end power laws and exponential expansions will be used below.

Case 1. Aging flow model $\eta_q = \eta_F(t)$ (2.24)

In this case we have to assign a definite structure to the flow rate $\Psi(\tau)$ and choose a power law which predicts unbounded creep for long duration of loading. Clearly, other functions could also be used for parametrization, such as hyperbolic or exponential laws, which would predict bounded creep capacity if only a small number of terms is used. Recalling (2.27), the unit creep function $g(t)$ is approximated directly by the following power law:

$$\eta_q(t)|_{\sigma=1} = g(t) = bt^m \ , \tag{3.29}$$

which is now evaluated at M sampling points in terms of the optimization variable b

$$f(x_j) = b(t_k^m - t_l^m) \ , \quad k = 1, 2, \ldots 14 \ ; \ l = 1, 2 \ldots 4 \ . \tag{3.30}$$

The optimum parameter value is readily identified for different powers $m_r = m_{r-1} + 0.025$ yielding a global optimum for

$$m = 0.025 \ , \quad b = 601 \ , \quad \text{with} \quad \boldsymbol{\delta_M} = \mathbf{0.238} \quad N = 1 \ , \quad M = 56 \ . \tag{3.31}$$

The "best" approximation of an aging flow model – rate of creep method – is shown in fig. 3.8. It illustrates very clearly that the creep response is underestimated considerably at high ages of loading. Moreover, this model would predict no creep recovery if the specimen were unloaded, because of the irreversible flow mechanism.

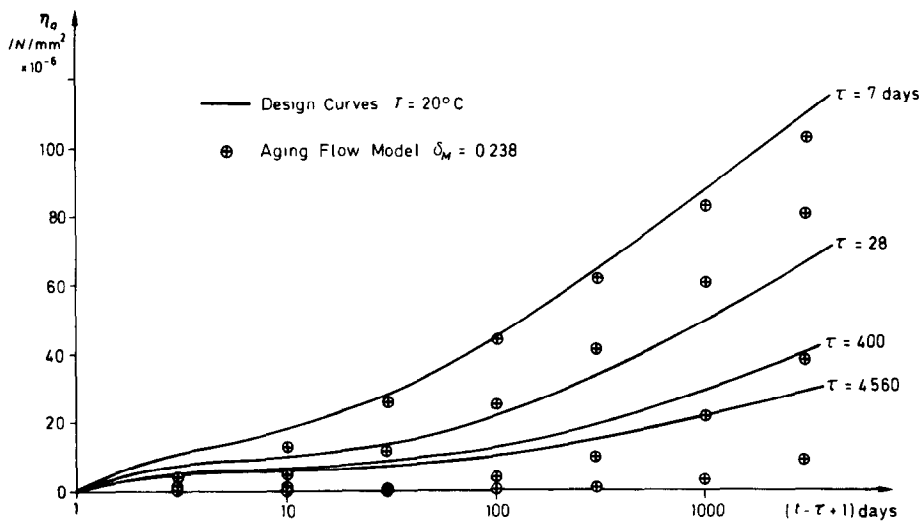

Fig. 3.8. Aging flow model of reduced creep surface $\eta_q = \eta_F(t)$.

Case 2. Delayed elastic model $\eta_q = \eta_D(t - \tau)$ (2.28)

In this case, identification follows essentially along the line of a non-aging Kelvin chain yielding a global optimum at $n = 6$ for the present data. The parameters are

i	λ_α	$\mathcal{J}_\alpha$	
1	3.0	3.14	
2	0.3	2.56	$N = 5$
3	0.03	0.174	$M = 56$
4	0.003	0.074	$\boldsymbol{\delta_M} = \mathbf{0.474}$
5	0.0003	0.011	

(3.32)

The "best" fit of a delayed elastic model with no aging is shown in fig. 3.9. It illustrates very

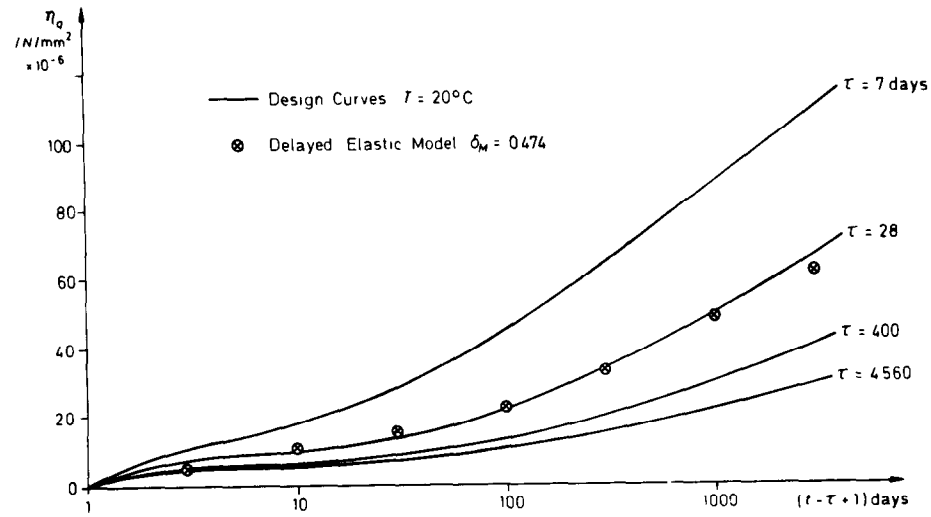

Fig. 3.9. Delayed elastic model of reduced creep surface $\eta_{q'} = \eta_D(t - \tau)$.

clearly that the doubly curved creep surface is in this case approximated by a cylindrical surface which averages the effect of aging. For this reason the creep capacity is underestimated for loading of very young concrete and overestimated for very old concrete. Moreover, the delayed elastic model would predict complete creep recovery if the specimen were unloaded.

Case 3. Summation model $\eta_q = \eta_F(t) + \eta_D(t - \tau)$ (2.33)

In this case, identification involves the evaluation of two functions for flow and a delayed elasticity, in a manner similar to the previous two cases. If the number of exponential terms and the power of the flow expansion are treated as optimization variables, a considerable number of feasible combinations has to be examined. Starting with initial values from the aging flow model, a global optimum is quickly found at

$$n = 5\,, \quad m = 0.025\,, \quad b = 471\,, \quad \text{with} \quad \boldsymbol{\delta}_M = 0.147\,. \tag{3.33}$$

The associated parameter values are

i	λ_α	$\mathcal{J}_\alpha$	
1	3.0	11.7	
2	0.3	0.865	$N = 6$
3	0.03	0.0	$M = 56$
4	0.003	0.019	
5	0.0003	0.0018	

(3.34)

The "best" fit of the summation model – rate of flow method – is shown in fig. 3.10. It illustrates acceptable agreement between input curves and creep predictions for the entire response spectrum, i.e. loading durations up to 3000 days and loading ages which vary from 7 to 4560 days. In the case of unloading, the summation model would predict partial recovery due to delayed action while the

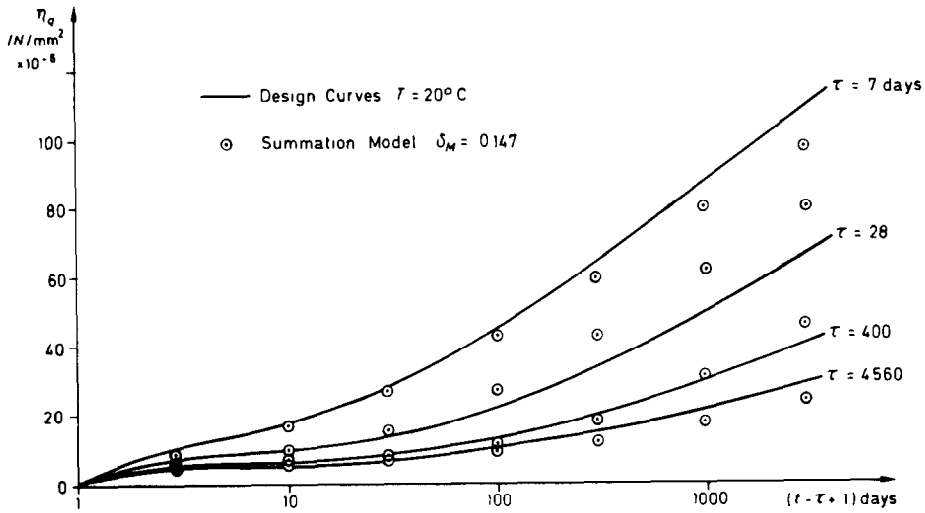

Fig. 3.10. Summation model of reduced creep surface $\eta_q = \eta_F(t) + \eta_D(t - \tau)$.

irreversible component would be controlled by permanent flow analogous to the Burgers model.

Case 4. Product model $\eta_q = \eta_D(\tau, t - \tau)$ (2.36)

As in the case of the summation model, two functions must be identified, since the creep rate is now a product of two functions; one describes the variation from the time of loading within the frame work of a delayed model, while the other defines the effect of loading age. The resulting homothetic law forms the kernel of eq. (2.37), in which the aging function has to be parametrized. To this end we choose the following exponential expansion [1]

$$\Phi(\tau) = \sum_{\beta=1}^{n_\beta} A_\beta^2 \exp(-\lambda_\beta \tau) , \tag{3.35}$$

which describes a monotonically decreasing function of age analogous to the approximation of the elastic component (3.6). For a unit stress history we are able to integrate eq. (2.39) and express the unit creep surface in terms of the free parameters A_α, A_β:

$$\eta_D(\tau, t - \tau)|_{\sigma=1} = \sum_{\alpha=2}^{n_\alpha} \sum_{\beta=1}^{n_\beta} \frac{A_\alpha^2 A_\beta^2}{\lambda_\alpha - \lambda_\beta} [\exp(-\lambda_\beta t) - \exp(-\lambda_\alpha (t - \tau)) \exp(-\lambda_\beta \tau)] . \tag{3.36}$$

The aging function $\Phi(\tau)$ has to cover the entire range of loading, thus the number of exponential terms $n_\beta \geqslant 4$. In our case $n_\beta = 5$ was used for the series expansion, which includes a constant for $n_\beta = 1$ where $\lambda_\beta = 0$. Treating the number of exponential terms n_α as optimization variables and evaluating (3.36) at M sampling points in terms of A_α, A_β:

$$f(x_j) = \sum_{\alpha=2}^{n_\alpha} \sum_{\beta=1}^{5} \frac{A_\alpha^2 A_\beta^2}{\lambda_\alpha - \lambda_\beta} [\exp(-\lambda_\beta t_k) - \exp(-\lambda_\alpha (t_k - t_l)) \exp(-\lambda_\beta t_l)] , \tag{3.37}$$

where $j = 1, 2, \ldots M = 56$ and $k = 1, \ldots 14$; $l = 1, \ldots 4$,

we obtain an optimum via the least squares procedure at

$$n_\alpha = 8\,, \quad n_\beta = 5\,, \quad \text{with} \quad \boldsymbol{\delta}_M = 0.176\,. \tag{3.38}$$

The resulting parameter values are

i	$\lambda_\alpha = \lambda_\beta$	A_α^2	A_β^2	
1	0	–	0.002	
2	3	4.930	1.000	
3	0.3	0.005	8.000	
4	0.03	0.0	0.128	$N = 12$
5	0.003	0.0	0.023	$M = 56$
6	0.0003	1.030	–	
7	0.00003	2.920	–	
8	0.000003	1.560	–	

(3.39)

The "best" fit of the product model is shown in fig. 3.11. A comparison with the results of the non-aging Klevin chain, fig. 3.9, illustrates the improvement due to the aging function $\Phi(\tau)$. For load durations up to 300 days there is a tendency to underestimate the creep response at high loading ages, very much like the aging flow model. In the case of unloading, the product model would predict partial creep recovery similar to the summation model, except that reversible and irreversible contributions are not separated explicitely.

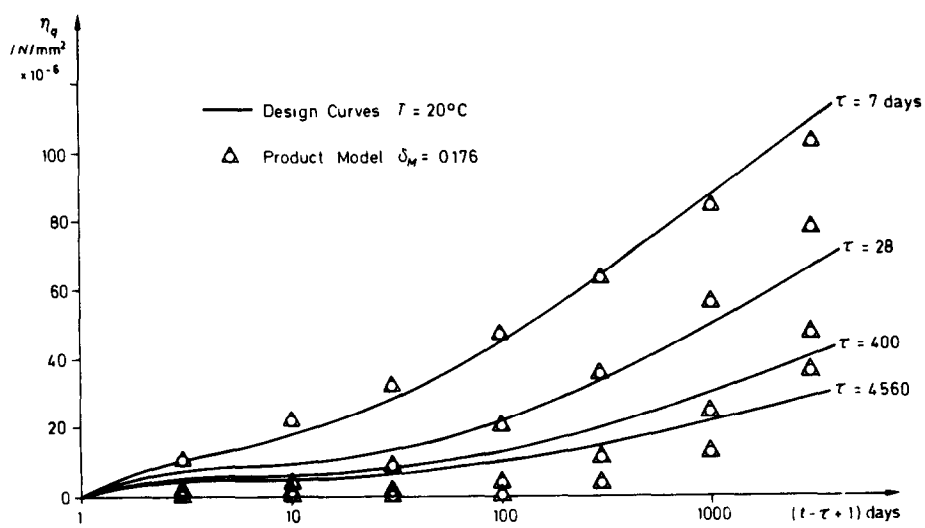

Fig. 3.11. Product model of reduced creep surface $\eta_q = \eta_D(\tau, t - \tau)$.

Case 5. Effective time model $\eta_q = \eta_D(\xi_t - \xi_\tau)$ (2.40)

In this case, identification involves again two functions, the time shift function ξ_t in eq. (2.42) and the delayed component. The effective time transformation is parameterized here by a power function

$$\xi_t = ct^m \ , \tag{3.40}$$

which is introduced into eq. (2.45) to evaluate the unit creep function at M sampling points in terms of the unknown parameters c and A_α:

$$f(x_j) = \eta_D(\xi_k - \xi_l)|_{\sigma=1} = \sum_{\alpha=2}^{n} \frac{A_\alpha^2}{D_\alpha} [1 - \exp(-D_\alpha(\xi_k - \xi_l))] \ . \tag{3.41}$$

For identification we treat the number of exponential terms as optimization variables and examine feasible combinations with different powers $m_r = m_{r-1} + 0.025$. A global optimum is attained at

$$m = 0.15, \quad n = 5 \ , \quad \text{with} \quad \delta_M = 0.172 \ . \tag{3.42}$$

Amplitudes for the exponential expansion are

i	D_α	A_α^2
1	3	26.50
2	0.3	0
3	0.03	0
4	0.003	0
5	0.0003	0.51

$N = 6$
$M = 56$ (3.43)

The "best" fit of the time shift model is shown in fig. 3.12. A comparison with predictions of the non-aging Kelvin chain in fig. 3.9 illustrates that the overall approximation is improved considerably by the age-compensating transformation of time $\xi = \xi(t)$. In the case of unloading the effective time model would predict partial creep recovery similar to the summation model, except that reversible and irreversible contributions are not separated from the beginning.

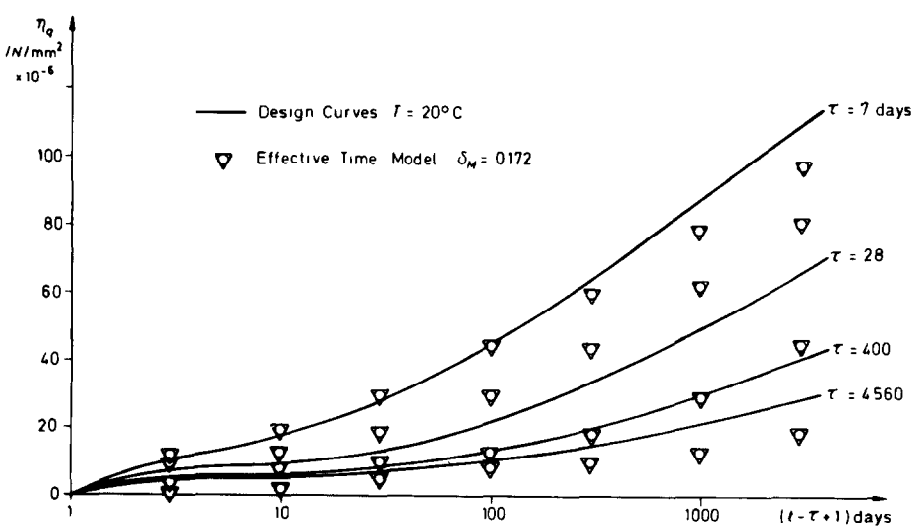

Fig. 3.12. Effective time model of reduced creep surface $\eta_q = \eta_D(\xi_t - \xi_\tau)$.

Summary

Before proceeding to concrete creep under higher temperatures let us summarize the previous findings on aging and its identification.

From the creep data, fig. 3.4, we have seen that the effect of loading varies strongly with time. Between 7 and 28 days the creep capacity (i.e. the elastic and the hereditary components) is largely reduced. Between 28 to 400 days only the hereditary components decrease slowly, while between 500 and 5000 days the elastic contribution decreases faster then the hereditary component. Considering the large differences in aging of the individual deformation components, we could conceivably confine attention to small portions of the aging spectrum. In this way the age effect would be eliminated at the cost of severe restrictions on the range of application. On the other hand, if the creep model has to apply to a wide range of loading histories, then aging of the individual deformation components has to be considered. Accordingly, the structure and performance of the previous models are summarized in the table (3.44).

Creep model	Deformation	Aging	Recovery	Optimization variables N	RMS error $\delta_M = \Delta_M / Y_M$
Maxwell	$\gamma = \epsilon + \eta_F$	No	No	2	0.359 (i)
Kelvin	$\gamma = \epsilon + \eta_D$	No	Full	6	0.335
Burgers	$\gamma = \epsilon + \eta_F + \eta_D$	No	Partial	6	0.335
Hyperelastic	$\epsilon(t)$	Yes	Partial	6	0.028 (ii)
Delayed elastic	$\eta_q = \eta_D(t - \tau)$	No	Full	5	0.474 (iii)
Aging flow	$\eta_q = \eta_F(t)$	Yes	No	1*	0.238
Summation	$\eta_q = \eta_F(t) + \eta_D(t - \tau)$	Yes	Partial	6*	0.147
Product	$\eta_q = \eta_D(\tau, t - \tau)$	Yes	Partial	12	0.176
Time shift	$\eta_q = \eta_D(\xi_t - \xi_\tau)$	Yes	Partial	6*	0.172

(i) γ-Norm $Y^{\gamma}_{56} = 67.69 * 10^{-6}$ per N/mm^2
(ii) η-Norm $Y^{\epsilon}_{6} = 35.33 * 10^{-6}$ per N/mm^2
(iii) η-Norm $Y^{\eta}_{56} = 36.16 * 10^{-6}$ per N/mm^2

(3.44)

The root mean square error δ_M describes the relative accuracy of the creep approximation at $M = 54$ sampling points as compared to the input data; N denotes the number of optimization variables representing the identification effort. For creep models with an asterisk "*", N has to be multiplied by the number of trials which are necessary to find the optimum exponent of the power expansion.

The relative RMS errors δ_M in eq. (3.44) are on one hand a measure for the accuracy of each parameterization; on the other hand, they contain model bias [30], i.e. approximation errors which are introduced by the specific mathematical structure and which do not vanish with increasing number of model parameters. In our particular case the largest part of δ_M reflects model bias because the number of terms in the exponential expansion is an optimization variable.

For creep under variable stress, and in particular for load-unload regimes, the summation law is very convenient since reversible and irreversible deformation components are described separately by delayed elastic and flow action. They are readily identified from creep and recovery data but unfortunately they are not available for the particular Wylfa concrete. In spite of these reservations the previous summation model will be extended below elevated temperature regimes.

3.5. Creep model for elevated temperature

Recalling the test data shown in fig. 3.5 for $T = 95°C$, we readily construct a design curve for the hereditary deformation component η_q by subtracting the instantaneous elastic contribution from total strain:

$$\text{for } T = 95°C: \quad \eta_q(t) = \gamma(t) - \epsilon(t) . \tag{3.45}$$

As a result, we obtain the age-independent creep curve shown in fig. 3.13 for which the summation model is readily identified using the least squares procedure above. For compatibility with the best fit at $T = 20°C$, where

$$m = 0.025 , \quad n = 5 , \quad b = 0 , \quad \text{with} \quad \boldsymbol{\delta_M = 0.005} , \tag{3.46}$$

the following parameter values are found by Marquardt optimization:

i	λ_α	α
1	3.0	34.5
2	0.3	8.13
3	0.03	0.672
4	0.003	0.067
5	0.0003	0.0073

$N = 6$
$M = 56$ (3.47)

Thus, the least squares procedure predicts zero flow and describes, as expected, the non-aging time variation exclusively by delayed elastic action.

The "best" fit to the summation model is shown in fig. 3.13, illustrating very close agreement with the given input data. Recalling our previous experience with the non-aging Kelvin chain and Burgers model, differences arose only when the exponential series was restricted to very few terms. Clearly, with $n = 5$ there are sufficient degrees of freedom so that the flow component is not even activated in eq. (3.46). However, the resulting non-aging Kelvin chain predicts full creep recovery when unloaded at 95°C – this must be questioned in the light of experimental evidence as e.g. reported in [5, 8]. In the following the proposed creep model will be applied to temperature histories with $T \leqslant 70°C$; thus the irreversible flow component does not vanish in this case. However, we keep in mind that the present temperature model must be revised as soon as additional thermal load-unload data become available.

Let us now examine temperatures other than $T = 20°$ and 95°C, still retaining isothermal conditions. Additional creep data at intermediate temperature were published previously [25] for the Wylfa concrete, but experimental scatter and discrepancies with recent data [24] furnish little conclusive evidence. Therefore, the simplest approach is adopted, namely linear interpolation of creep deformations at $T = 20°$ and $T = 95°C$, even though some researchers have made different observations [31]. To this end we scale the coefficients of each creep component linearly with temperature:

$$\text{for } 20° < T < 95°: \; \mathcal{J}^*_\alpha(T) = \mathcal{J}_\alpha(T_{20}) + \Delta\mathcal{J}_\alpha \overline{T}$$

$$\text{where } \overline{T} = (T - 20)/75 \text{ and } \Delta\mathcal{J}_\alpha = \mathcal{J}_\alpha(T_{95}) - \mathcal{J}_\alpha(T_{20}) . \tag{3.48}$$

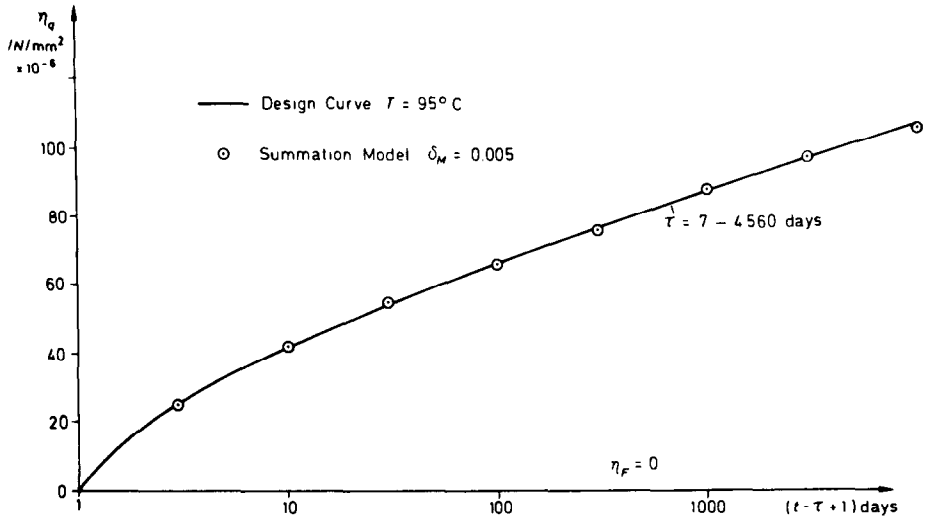

Fig. 3.13. Summation model of reduced creep surface $\eta_q = \eta_F(t) + \eta_D(t - \tau)$.

From the least squares identification of the elastic component eq. (3.6) we obtain for a unit stress input at time t and temperature T:

$$\epsilon(t, T)|_{\sigma=1} = \sum_{i=1}^{6} a_i^*(T) \exp(-c_i t) , \tag{3.49}$$

where the temperature-dependent amplitudes $a_i^*(T)$ are

$$a_i^*(T) = a_i(T_{20}) + [a_i(T_{95}) - a_i(T_{20})]\ \overline{T} , \tag{3.50}$$

and the values at $T = 20°$ and 95°C are given in eq. (3.10).

From the previous identification of the summation model at $T = 20°$ and 95° the temperature variation of the flow component is readily constructed

$$\eta_F(t, T)|_{\sigma=1} = b^*(T) t^{0.025} . \tag{3.51}$$

By eqs. (3.33), (3.46), coefficient $b^*(T)$ is given by

$$b^*(T) = 471 - 471\overline{T} . \tag{3.53}$$

Therefore, the time variation of the flow compliance decreases with increasing temperature and reaches zero at $\eta_F(t, T_{95}) = 0$.

In analogy the associated delayed elastic component for elevated temperatures is given by

$$\eta_D(t - \tau, T)|_{\sigma=1} = \sum_{\alpha=2}^{6} \frac{\mathcal{J}_\alpha^*(T)}{\lambda_\alpha} [1 - \exp(-\lambda_\alpha(t - \tau))] . \tag{3.52}$$

From eqs. (3.34), (3.47) we obtain the temperature-dependent amplitudes

$$\mathcal{J}_\alpha^*(T) = \mathcal{J}_\alpha(T_{20}) + [\mathcal{J}_\alpha(T_{95}) - \mathcal{J}_\alpha(T_{20})]\,\bar{T}\,. \tag{3.54}$$

In this case the time variation of delayed elaticity increases considerably with increasing temperature. The temperature dependence of the individual deformation components is illustrated below in section 5, where the creep law is applied to predict the behaviour of a PCRV.

In conclusion we note that expressions (3.49), (3.51), (3.53) describe the creep behaviour for different but *constant* temperatures, i.e. isothermal conditions with vanishing temperature rates. To extend the creep model to variable temperature histories, an additional postulate is required. In the past, more from convenience then experimental confirmation, it has been assumed that the creep rate depends on temperature but not on temperature rate or time derivatives of higher order.

The time rate of change of e.g. the flow mechanism (3.51) is controlled by two terms:

$$\eta_F(t, T)|_{\sigma=1} = b^*(T)t^m \tag{3.55}$$

and

$$\dot{\eta}_F(t, T)|_{\sigma=1} = b^*(T)mt^{m-1} + \underbrace{\frac{\partial b^*(T)}{\partial T}\,t^m\,\dot{T}}_{\text{transitional thermal creep}}\,, \tag{3.56}$$

where the second term depends on the temperature rate, an effect which is normally neglected.

Only recently, "transitional" creep effects have been reported [8, 26] which considerably enhance irreversible creep deformations when the temperature is raised on a virgin specimen *after* the mechanical load has been applied. Clearly, the internal variable model readily describes such phenomena by an additional flow mechanism along the line of (3.56), which progresses only under increasing temperatures, i.e. positive temperature rates above a certain temperature level. This discontinuous process could be controlled by a temperature step function $\langle T - T_F \rangle$ analogous to the yield condition in plasticity. For the time being, temperature rate effects are not incorporated in the creep model because conclusive experimental evidence is still lacking for the Wylfa concrete under consideration.

4. Numerical solution method

In the following an incremental algorithm is developed for the numerical solution of creep integral eq. (2.21). In a given time interval the evolution of individual deformation components is described by a single-step recursion formula without resorting to previous history. The creep strains are referred to an elastic modulus E_0 which remains constant along the lines of the initial strain concept. Subsequently, the one-dimensional creep law is extended to triaxial conditions and then projected onto the structural level via finite elements. The resulting numerical scheme advances the creep process by the solution of additional load cases.

4.1. Incremental algorithm

In (2.21) the total deformation is composed of instantaneous and hereditary components

$$\gamma(t) = \underbrace{\epsilon(t) + \eta_T(t) + \eta_H(t)}_{\text{instantaneous}} + \underbrace{\eta_F(t) + \eta_D(t)}_{\text{hereditary}} . \tag{4.1}$$

Sampling (4.1) at both ends of the time interval $\Delta_j(t)$ yields the values for the corresponding incremental relationship

$$\Delta_j\gamma = \Delta_j\epsilon + \Delta_j\eta_T + \Delta_j\eta_H + \Delta_j\eta_F + \Delta_j\eta_D , \tag{4.2}$$

where in time step $\Delta_j(t)$ the flow component is given by

$$\Delta_j\eta_F = \eta_F(t_{j+}) - \eta_F(t_{j-}) . \tag{4.3}$$

Using the elastic properties at reference age t_0, the stress increment during time interval $\Delta_j(t)$ is given by

$$\Delta_j\sigma = \frac{1}{E_0}\,\Delta_j\epsilon = \frac{1}{E_0}\,[\Delta_j\gamma - \Delta_j\eta] . \tag{4.4}$$

The initial strain increment $\Delta_j\eta$ is composed of mechanical and environmental (thermal/hygral) components. Because of aging, the mechanical term in general also contains an elastic contribution in addition to flow and delayed components

$$\Delta_j\eta_c = \Delta_j\eta_E + \Delta_j\eta_F + \Delta_j\eta_D . \tag{4.5}$$

For isothermal/isohygral conditions at reference temperature/humidity

$$\Delta_j\eta_T = \Delta_j\eta_H = 0 , \tag{4.6}$$

and for non-aging elastic response behaviour

$$\Delta_j\eta_E = 0 . \tag{4.7}$$

Let us now briefly examine individual initial strain contributions which are summarized in the appendix for the Wylfa concrete using the summation model.

1. Elastic component: $\epsilon(t) = \dfrac{1}{E[T(t), H(t), t]}\,\sigma(t)$ (2.15)

Note the change of elastic properties in the hyperelastic formulation (2.15) due to aging or equivalent temperature/humidity effects. In a time interval Δt_j the increments of stress and elastic strains are related by

$$\Delta_j\sigma = E(t_j)\,\Delta_j\epsilon + \underbrace{\Delta_j E(t_j)\epsilon}_{\text{higher order}} . \tag{4.8}$$

For computational convenience the initial elastic modulus E_0 is used as reference value throughout the entire creep process (eq. (4.4)). Therefore, the right-hand side of eq. (4.8) is augmented by an additional initial strain contribution η_E to correct the time-invariable stress-strain law for aging elastic behaviour:

$$\Delta_j\sigma = E_0(\Delta_j\epsilon + \Delta_j\eta_E)\,. \tag{4.9}$$

For equivalence with (4.8) the initial strain correction is for aging elastic behaviour:

$$\Delta_j\eta_E = \frac{E_0 - E(t_j)}{E(t_j)E_0}\,\Delta_j\sigma\,. \tag{4.10}$$

2. *Flow component:* $$\eta_F(t) = A_1^2 \int_{t_0}^{t} \Psi[T(\tau), H(\tau), \tau]\ \sigma(\tau)\,\mathrm{d}\tau \tag{2.26}$$

Invoking the mean value theorem of integration, we obtain for the flow increment

$$\begin{aligned}\Delta_j\eta_F &= A_1^2\,\sigma(t_j^*) \int_{t_{j-}}^{t_{j+}} \Psi[T(\tau), H(\tau), \tau]\ \mathrm{d}\tau \\ &= A_1^2\,\sigma(t_j^*)\,\Psi[T(t_j^*), H(t_j^*), t_j^*]\,\Delta t_j\,, \qquad t_{j-} \leqslant t_j^* \leqslant t_{j+}\,.\end{aligned} \tag{4.11}$$

At reference temperature/humidity and for a flow mechanism which does not age, $\Psi = 1$, and thus (2.27) degenerates to a simple time-marching algorithm with constant viscosity

$$\Delta_j\eta_F = A_1^2\,\sigma(t_j^*)\,\Delta_j t\,. \tag{4.12}$$

3. *Delayed component:* $$\eta_D(t) = \sum_{\alpha=2}^{n} A_\alpha^2 \int_{\xi_0}^{\xi} \exp(-D_\alpha(\xi_t - \xi_\tau))\,\sigma(\xi_\tau)\,\mathrm{d}\xi_\tau \tag{2.44}$$

In the effective time model, aging of the delayed component is described by a nonlinear transformation of the time scale in the form of

$$\xi_t = \int_{t_0}^{t} \Phi[T(s), H(s), s]\,\mathrm{d}s\,, \qquad \xi_\tau = \int_{t_0}^{t} \Phi[T(s), H(s), s]\,\mathrm{d}s\,. \tag{2.42}$$

Sampling (2.44) at both ends of the variable time interval Δt_j yields the following expression for the delayed increment:

$$\Delta_j\,\eta_D = \sum_{\alpha=2}^{n} [\mu_j + \Delta_j\mu]_\alpha\,. \tag{4.13}$$

This single-step recursion formula determines the value of μ at t_j in terms of the value at t_{j-1} and $\Delta_{j-1}\mu$:

$$\mu_j = [\exp(-D_\alpha \Delta_j \xi) - 1]\left[\frac{\exp(-D_\alpha \Delta_{j-1}\xi)}{\exp(-D_\alpha \Delta_{j-1}\xi) - 1}\mu_{j-1} + \Delta_{j-1}\mu\right] \tag{4.14}$$

and

$$\Delta_j \mu = \frac{A_\alpha^2 \sigma(t_j^*)}{D_\alpha}(1 - \exp(-D_\alpha \Delta_j \xi)\,, \quad t_{j-} \leqslant t_j^* \leqslant t_{j+}\,.$$

The effective time increment derives from the mean value theorem of integration

$$\Delta_j \xi = \int_{t_{j-}}^{t_{j+}} \Phi[T(s), H(s), s]\,\mathrm{d}s = \Phi[T(t_j^*), H(t_j^*), t_j^*]\,\Delta_j t\,. \tag{4.15}$$

At reference temperature/humidity and for non-aging delayed action, $\Phi = 1$ and

$$\Delta_j \xi = \Delta_j t\,. \tag{4.16}$$

In this case real time replaces effective time in recursion formula (4.14) along the lines of the delayed elastic model (2.28) and the summation model (2.33):

$$\begin{aligned} \mu_j &= [\exp(-\lambda_\alpha \Delta_j t) - 1]\left[\frac{\exp(-\lambda_\alpha \Delta_{j-1} t)}{\exp(-\lambda_\alpha \Delta_{j-1} t) - 1}\mu_{j-1} + \Delta_{j-1}\mu\right], \\ \Delta_j \mu &= \frac{\mathcal{J}_\alpha \sigma^*(t_j)}{\lambda_\alpha}(1 - \exp(-\lambda_\alpha \Delta_j t))\,. \end{aligned} \tag{4.17}$$

Aging in the form of the homothetic product expansion leads to a recursion expression which is similar to (4.17) except for additional weighting due to aging.

4. Thermal strain: $\eta_T(t) = \alpha[T(\tau), H(\tau), \tau]\; T(t)$ (2.15)

The change of thermal strain in the time increment $\Delta_j t$ is readily obtained assuming that the contribution due to the change of thermal expansion is of higher order:

$$\Delta_j \eta_T = \alpha[T(t_j^*), H(t_j^*), t_j^*]\;\Delta_j T + \ldots\,. \tag{4.18}$$

For constant thermal expansion α_0 we recover the customary initial strain increment due to a change in temperature

$$\Delta_j \eta_T = \alpha_0 \Delta_j T\,. \tag{4.19}$$

5. Hygral strain: $\eta_H(t) = \beta[T(\tau), H(\tau), \tau]\ H(t)$ (2.15)

The change of shrinkage strain in the time interval $\Delta_j t$ is again derived assuming that the contribution due to the change of hygral expansion is of higher order:

$$\Delta_j \eta_H = \beta[T(t_j^*), H(t_j^*), t_j^*]\ \Delta_j H + \dots . \tag{4.20}$$

For constant hygral expansion β_0 we recover the customary shrinkage strain increment due to a change in humidity

$$\Delta_j \eta_H = \beta_0 \Delta_j H . \tag{4.21}$$

4.2. Multiaxial conditions

Up to now the exposition has been confined to uniaxial stress conditions. Clearly, upon application to thick-walled concrete structures, creep predictions are needed for three-dimensional stress analysis, Therefore, additional assumptions have to be introduced to generalize the uniaxial stress-strain law to multiaxial conditions. Lacking conclusive experimental evidence, most concrete technologists [5, 32] support the simple hypothesis that all deformation components exhibit isotropic properties with Poisson's ratio equalling that of instantaneous elastic response. We adopt that hypothesis and note that the triaxial stress-strain law obeys the generalized Hooke's law

$$\boldsymbol{\varepsilon} = \boldsymbol{E}_0^{-1}\,\boldsymbol{\sigma} = \frac{1}{E_0}\boldsymbol{H}\,\boldsymbol{\sigma}\ , \tag{4.22}$$

where

$$\boldsymbol{H} = \begin{bmatrix} 1 & -\nu & -\nu & & & \\ -\nu & 1 & -\nu & & \boldsymbol{O} & \\ -\nu & -\nu & 1 & & & \\ & & & 2(1+\nu) & & \\ & \boldsymbol{O} & & & 2(1+\nu) & \\ & & & & & 2(1+\nu) \end{bmatrix} \tag{4.23}$$

is solely a function of Poisson's ratio, and the engineering definition of shear stress and strain is used with the following notation

$$\boldsymbol{\sigma} = \{\sigma_{11}, \sigma_{22}, \sigma_{33}, \sigma_{12}, \sigma_{23}, \sigma_{31}\}\ ; \qquad \boldsymbol{\varepsilon} = \{\epsilon_{11}, \epsilon_{22}, \epsilon_{33}, \epsilon_{12}, \epsilon_{23}, \epsilon_{31}\}\ . \tag{4.24}$$

The multiaxial creep strain increment $\Delta_j \boldsymbol{\eta}_c$ follows the derivation of the elastic component ex-except that the elastic compliance $1/E_0$ is replaced by the corresponding one-dimensional creep compliance composed of mechanical creep contributions defined in (4.9), 4.10), (4.12) and (4.13):

$$\Delta_j \mathcal{G}_c = \Delta_j \eta_c |_{\sigma=1} = [\Delta_j \eta_E + \Delta_j \eta_F + \Delta_j \eta_D]_{\sigma=1} \,. \tag{4.24}$$

In analogy to (4.22) we obtain

$$\Delta_j \boldsymbol{\eta}_c = \Delta_j \mathcal{G}_c \boldsymbol{H} \boldsymbol{\sigma}(t_j) \,, \tag{4.25}$$

which states that the creep strain increments are collinear with stress, and their length is determined by the increment of the creep compliance. Clearly, the change of inelastic work is a quadratic form in stress:

$$\Delta_j W_c = \boldsymbol{\sigma}^{\mathrm{t}} \Delta_j \boldsymbol{\eta}_c = \Delta_j \mathcal{G}_c \boldsymbol{\sigma}^{\mathrm{t}} \boldsymbol{H} \boldsymbol{\sigma} \,, \tag{4.26}$$

thus satisfying the dissipation inequality as long as $\Delta_j \mathcal{G}_c$ is non-negative.

An alternative generalization of creep to multiaxial conditions is based on the notion of creep potential $f(\boldsymbol{\sigma})$, such that

$$\Delta_j \boldsymbol{\eta}_c = \Delta_j \mathcal{G}_c \frac{\partial f}{\partial \boldsymbol{\sigma}^{\mathrm{t}}} \,, \tag{4.27}$$

which is analogous to the flow-rule in classical plasticity. If we postulate that the potential is a quadratic form in stress

$$f(\boldsymbol{\sigma}) = \tfrac{1}{2} \boldsymbol{\sigma}^{\mathrm{t}} \boldsymbol{H} \boldsymbol{\sigma} \,, \tag{4.28}$$

the creep law (4.25) is recovered. We should keep in mind that the concomitant identification involves the evaluation of the scalar functions $\mathcal{G}_c$ and the creep potential. Recall that metal creep is normally restricted to deviatoric components; in this case $f(\boldsymbol{\sigma})$ could be describe by the von Mises condition or the Tresca criterion. However, for concrete the hypothesis (4.28) has been widely accepted in view of the limited experimental evidence and the large amount of data scatter. Generalisations to anisotropic behaviour, though straightforward, are at best of formal interest for the time being, especially if we consider that creep is composed of several mechanisms.

For completeness, initial strain increments due to thermal/hygral expansion are required. For isotropic behaviour these environmental components are purely volumetric; thus for triaxial conditions

$$\begin{aligned} \Delta_j \boldsymbol{\eta}_T &= \Delta_j \eta_T \boldsymbol{E}_{3,3} \,, \\ \Delta_j \boldsymbol{\eta}_H &= \Delta_j \eta_H \boldsymbol{E}_{3,3} \,, \end{aligned} \tag{4.29}$$

where the corresponding uniaxial expressions are given in (4.18), (4.20). The diagonal matrix $\boldsymbol{E}_{3,3}$ is made up of a unit submatrix and zeros elsewhere:

$$\boldsymbol{E}_{3,3} = \begin{bmatrix} \boldsymbol{I}_3 & \boldsymbol{O}_3 \\ \boldsymbol{O}_3 & \boldsymbol{O}_3 \end{bmatrix}, \qquad \boldsymbol{I}_3 = \begin{bmatrix} 1 & 0 & 0 \\ 0 & 1 & 0 \\ 0 & 0 & 1 \end{bmatrix}. \tag{4.30}$$

4.3. Finite element initial load method

Simplicity of the method and recent advances in computer software developments have turned the finite element method into an engineering tool which is widely accepted for the analysis of complex structures. For typical applications in the present context we refer to reader to previous publications by the authors on finite element displacement analysis of concrete structures [33, 34, 35].

In our particular case, the initial load method is applied for tracing the entire creep process without altering the elastic stiffness of reference age t_0. The displacement method discretizes the equilibrium conditions for a structure, expressed below in incremental form

$$\boldsymbol{K}_0 \Delta_j \boldsymbol{r} = \Delta_j \boldsymbol{R} \,. \tag{4.31}$$

For a given load increment $\Delta_j \boldsymbol{R}$ the unknown displacement increment $\Delta_j \boldsymbol{r}$ is readily solved by a direct solution method (factorization of the structural stiffness $\boldsymbol{K}$ and forward reduction of $\boldsymbol{R}$ as well as backward substitution in $\boldsymbol{r}$). In a given time interval $\Delta_j t$ the load increment is in general made up of external contributions $\Delta_j \boldsymbol{R}_p$, such as pressure and environmental transients as well as initial loads $\Delta_j \boldsymbol{R}_J$, which drive the evolution of the creep process

$$\Delta_j \boldsymbol{R} = \Delta_j \boldsymbol{R}_p + \Delta_j \boldsymbol{R}_J \,. \tag{4.32}$$

We recall that on the structural level the initial load increment is made up of individual element contributions which are in general exposed to different temperature/humidity and stress conditions

$$\Delta_j \boldsymbol{R} \;=\; \sum_e \boldsymbol{a}_e^{\mathrm{t}} \Delta_j J_c \,. \tag{4.33}$$

The assembly matrix $\boldsymbol{a}_e$ assigns to each element degree of freedom the corresponding degree on the structural level. The initial load increment for an element $\Delta_j \mathcal{J}_c$ result from integration of the dissipative creep energy over the element volume

$$\Delta_j J_c = \int_V \boldsymbol{\gamma}^{\mathrm{t}} \boldsymbol{E}_0 \Delta_j \boldsymbol{\eta}_c \, \mathrm{d}V \,, \tag{4.34}$$

where the triaxial creep strain increment is defined in (4.25) and comprises contributions from aging elastic behaviour, flow and delayed action (see (4.24)).

Before turning to the solution of actual creep examples, we note that the choice of time step is of crucial importance for the stability of the incremental step-by-step procedure. The critical time step in controlled by the frequency content of the loading history (mechanical or environmental) in comparison to the retardation or relaxation spectrum in the creep model. Aside from these general observations the following rule should be observed:

$$\|\Delta_j \boldsymbol{\eta}\| < \|\boldsymbol{\varepsilon}(t_j)\| \,, \tag{4.35}$$

which can be used to predict the maximum length of subsequent time steps (extrapolation).

In summary, we observe that the proposed time-marching algorithm advances the creep process

at the expense of solving an additional load case. Because of the degenerate structure of the proposed creep model there is no need for storing previous histories of stress or deformation except for their current values.

5. Prestressed concrete reactor vessel

In the following a rather complex engineering problem is examined to illustrate numerical implementation of the creep model above. A typical THTR prestressed concrete reactor vessel subjected to a realistic reactor environment is considered [36]. Fig 5.1 shows the geometric configuration and the idealization with axisymmetric finite elements of the programming system SMART [35]. The vessel is exposed to the loading history of fig. 5.2, which involves mechanical prestress, pressure cycles with extended hold times, as well as environmental effects due to shrinkage and a temperature gradient of $\Delta T = 50°C$. For subsequant analysis we assume that there is no interaction

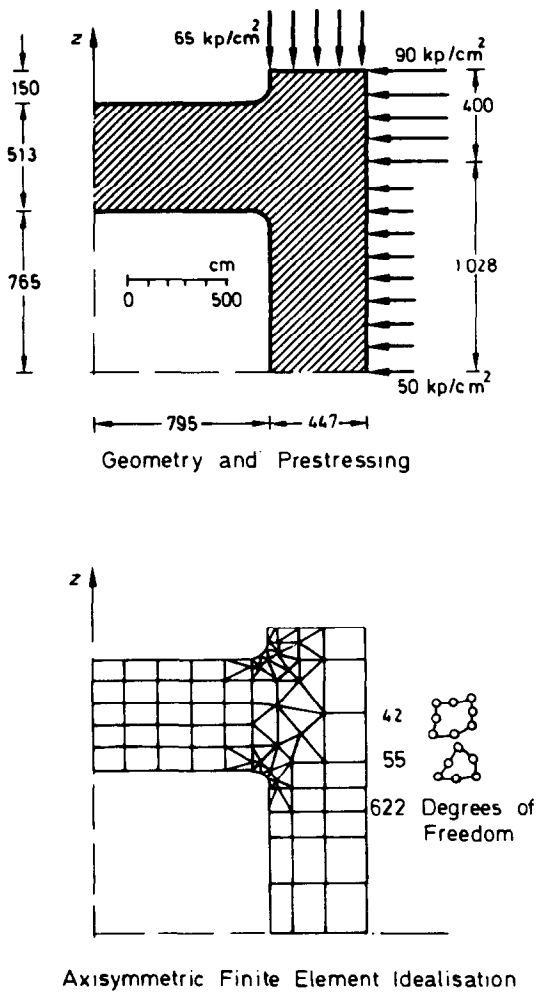

Fig. 5.1. Reference PCRV geometry and mesh layout.

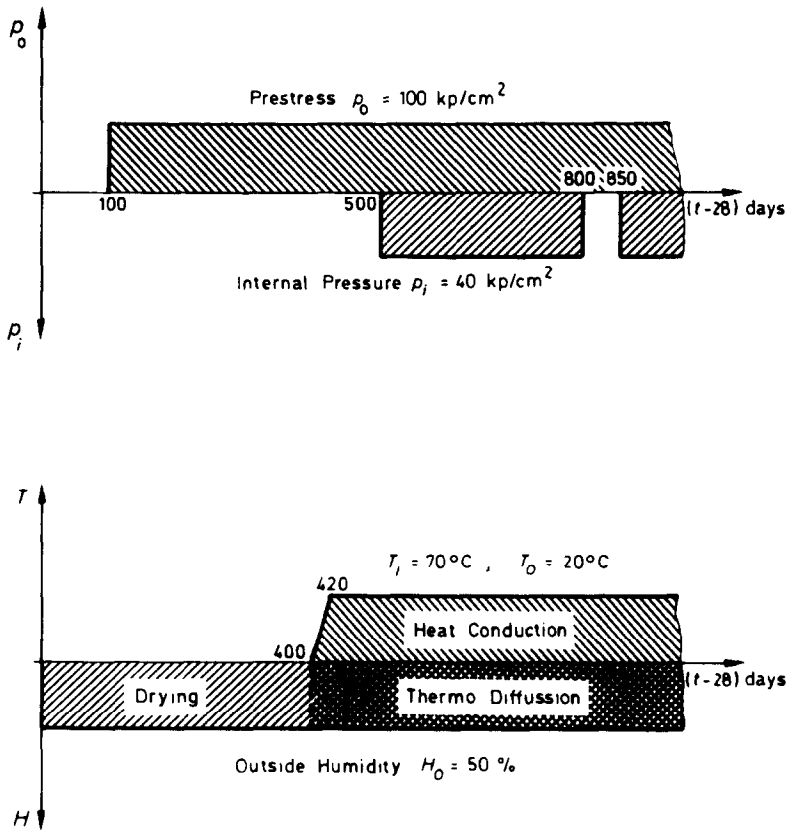

Fig. 5.2. Mechanical and environmental loading.

between the hygrothermal process of thermodifussion and the evolution of mechanical creep, i.e. moisture and thermal transport phenomena are uncoupled from stress and deformation. This customary hypothesis enables us to separate thermodiffusion analysis from stress analysis.

5.1. Hygrothermal solution

In the frist step we examine moisture transport in the concrete wall due to drying on the outside surface (moisture transfer to relative room hymidity H_0 = 50%) and due to the temperature gradient ΔT = 50°C across the containment wall. Clearly, the thermodiffusion problem is in general fully coupled; i.e. the thermal field influences the moisture field and vice versa. In order to simplify the concomitant identification problem which requires very complex testing [37]. we assume weak coupling between the two fields in the sense that only drying is affected by the temperature field, but thermal transport evolves independently of the moisture field. In this case the balance equation for transient humidity transport $\boldsymbol{H}(t)$ is governed by Fick's diffusion law augmented by a coupling term $\boldsymbol{L}_{HT}$ with the thermal field $\boldsymbol{T}(t)$ which accounts for temperature gradient effects. In matrix notation humidity transport in an idealized structure is controlled by [38]

$$\boldsymbol{C}_H\dot{\boldsymbol{H}} + \boldsymbol{K}_H\boldsymbol{H} = \boldsymbol{Q}_H + \boldsymbol{L}_{HT}\boldsymbol{T}\,. \tag{5.1}$$

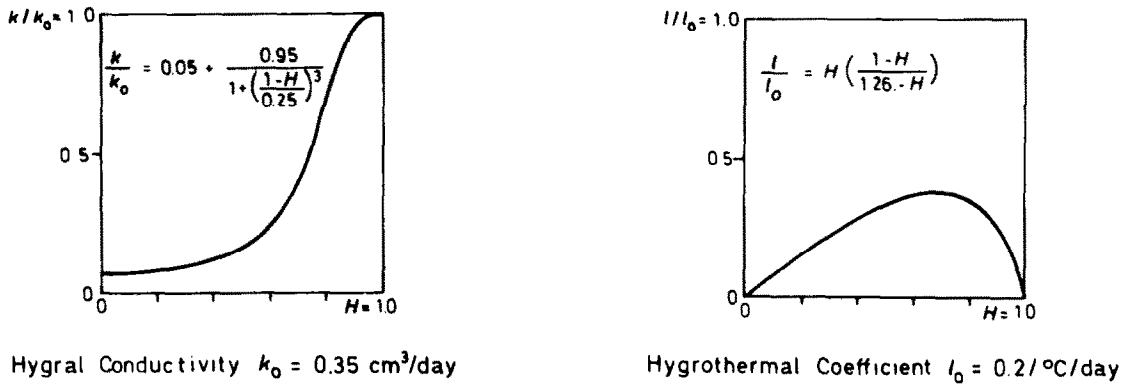

Fig. 5.3. Hygral diffusion properties, $C_H = 1$.

Thermal transport follows Fourier's law of heat conduction. Analogous to (5.1), heat transport is controlled by the following condition in which coupling with the humidity field is neglected:

$$C_T \dot{T} + K_T T = Q_T \,. \tag{5.2}$$

In this notation C and K define capacity and conductivity matrices of the finite element idealization, Q is the vector of nodal fluxes and L_{HT} denotes the hygrothermal coupling matrix, a term which was introduced in [38] for transient temperature environments. Augmenting the problem by initial and boundary values, both transient diffusion equations are readily solved in the case of weak coupling for the unknown humidity $H(t)$ and temperature $T(t)$ with the aid of an incremental step by step algorithm. They are converted subsequently into shrinkage and thermal strains as input for stress analysis. For further details of the thermodiffusion analysis see [39]; here we only note nonlinearities in form of moisture dependent conductivities $K(H)$, hygrothermal coupling $L_{HT}(H)$ and coefficients of expansion $\beta(H)$ as shown in figs. 5.3 and 5.4.

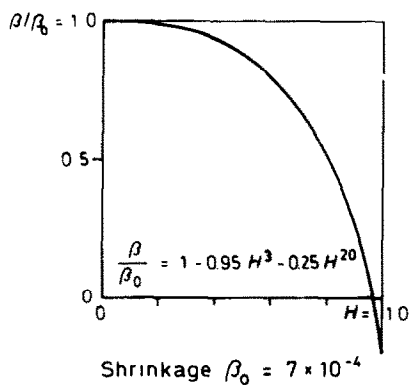

Fig. 5.4. Coefficient of hygral expansion.

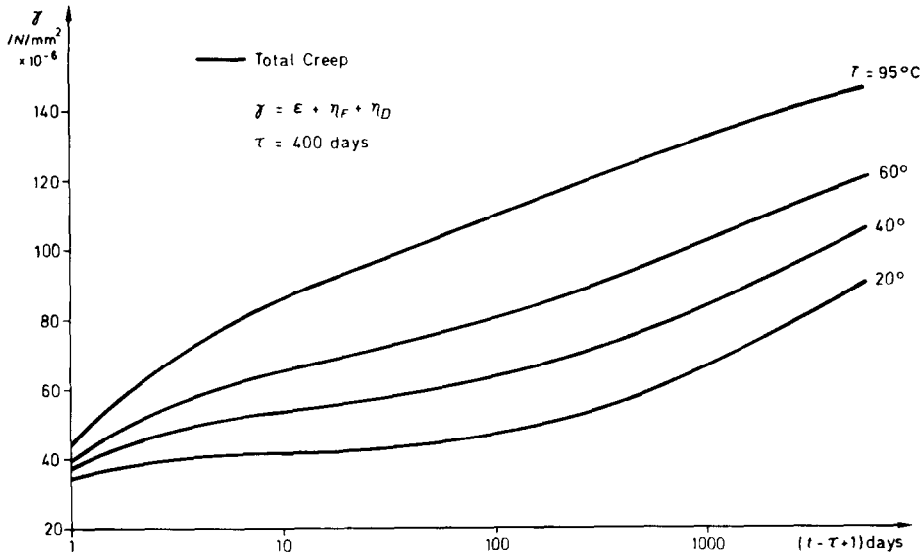

Fig. 5.5. Temperature dependence of total creep compliance.

5.2. Creep response behaviour

After solution of the environmental input history we proceed now with stress analysis for the combined loading presstress, pressure, shrinkage and temperature gradient. Constitutive behaviour is described by the temperature and age-dependent summation model of section 3.5, which, however, does not account for effects due to drying; i.e. the creep properties are in this case independent of humidity changes. The total creep compliance is illustrated in fig. 5.5 for the loading age $\tau = 400$ days with individual components shown in figs. 5.6, 5.7 and 5.8. For stress analysis we subdivide the entire loading history into time increments compatible with the step by step thermodiffusion solution above and apply the incremental initial load procedure described in section 4.3.

Considering loading without shrinkage, response histories are shown in fig. 5.9 for radial displacement and circumferential stress at point P. During prestress, up to 428 days, a state of pure creep

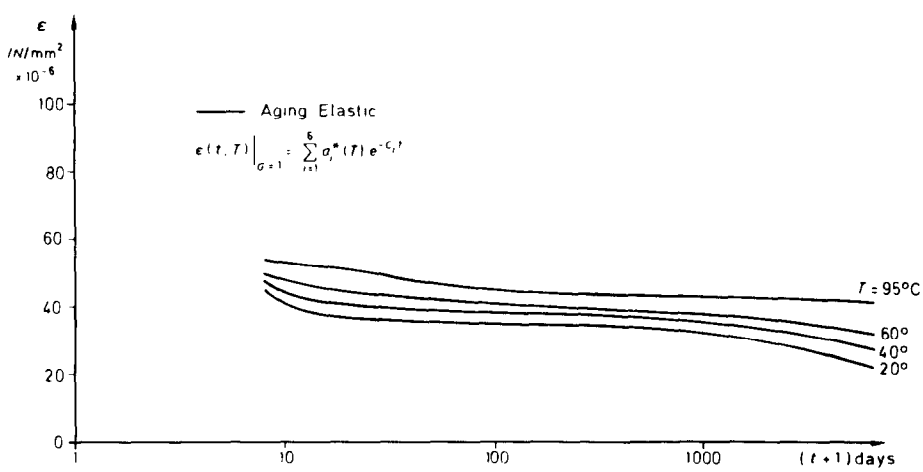

Fig. 5.6. Temperature dependence of elastic compliance.

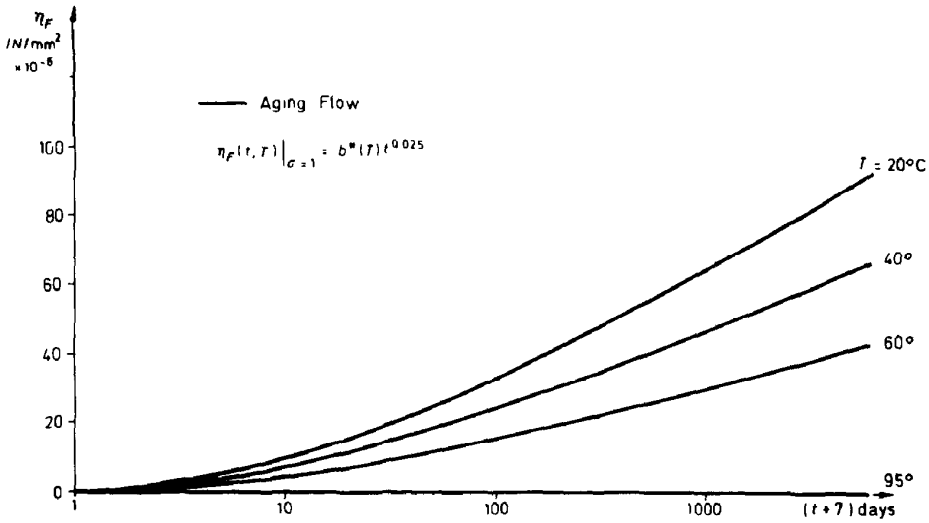

Fig. 5.7. Temperature dependence of flow compliance.

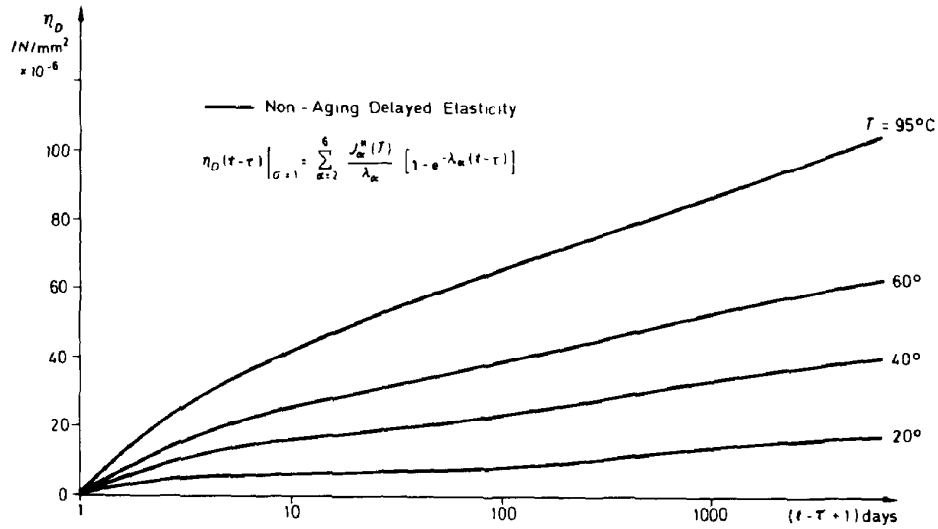

Fig. 5.8. Temperature dependence of delayed elastic compliance.

prevails in the wall without stress relaxation because of the homogeneous composition of this particular vessel and isothermal/isohygral conditions. Upon heating, stresses redistribute very quickly because of relaxation due to the temparature dependence of the creep function. Similar deformation response results from pressurization at 528 days, which counteracts stressing due to the temperature gradient across the wall. Pressure release from 828 to 878 days is almost reversible because of prevailing delayed elastic action. The corresponding response history is shown in fig. 5.10 for the case with shrinkage due to drying and thermodiffusion. Comparison with fig. 5.9 indicates that there is virtually no difference in deformation but a rather significant reduction of stress due to shrinkage at the inside wall caused by thermodiffusion after heating at 428 days.

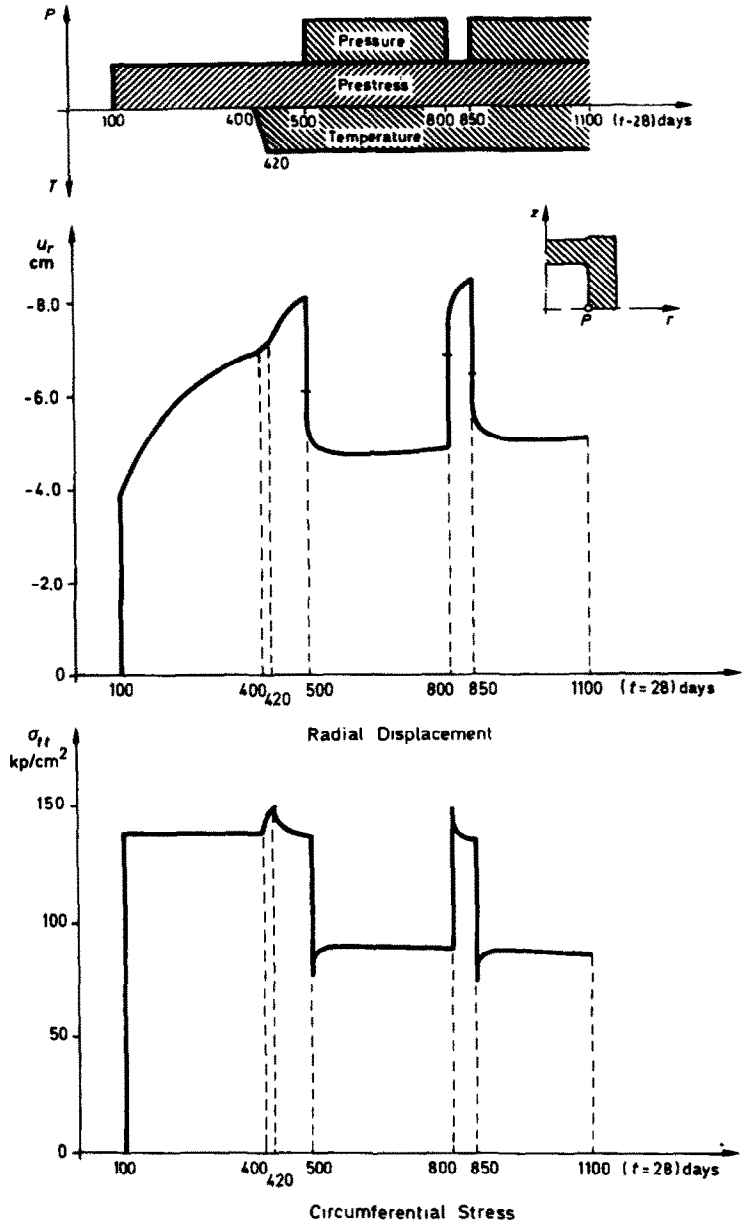

Fig. 5.9. Response history at point P, no shrankage.

To complete the discussion, circumferential stress distributions across the containment wall are shown in figs. 5.11 and 5.12 for loading histories with and without shrinkage. At 428 days, immediately after prestressing, stresses relax approximately 50 kp/cm² in a narrow zone near the outside surface, where the vessel is exposed to shrinkage due to drying. At 448 days, immediately after heating, thermal effects introduce a slight stress gradient. The relaxation effects are still confined to the outside because of the wall thickness and since drying due to thermodiffusion only starts at the time of heating. At 1128 days, that is during full operation, there is a considerable reduction of prestress level because of pressurization. Because of thermodifffusion, a narrow zone

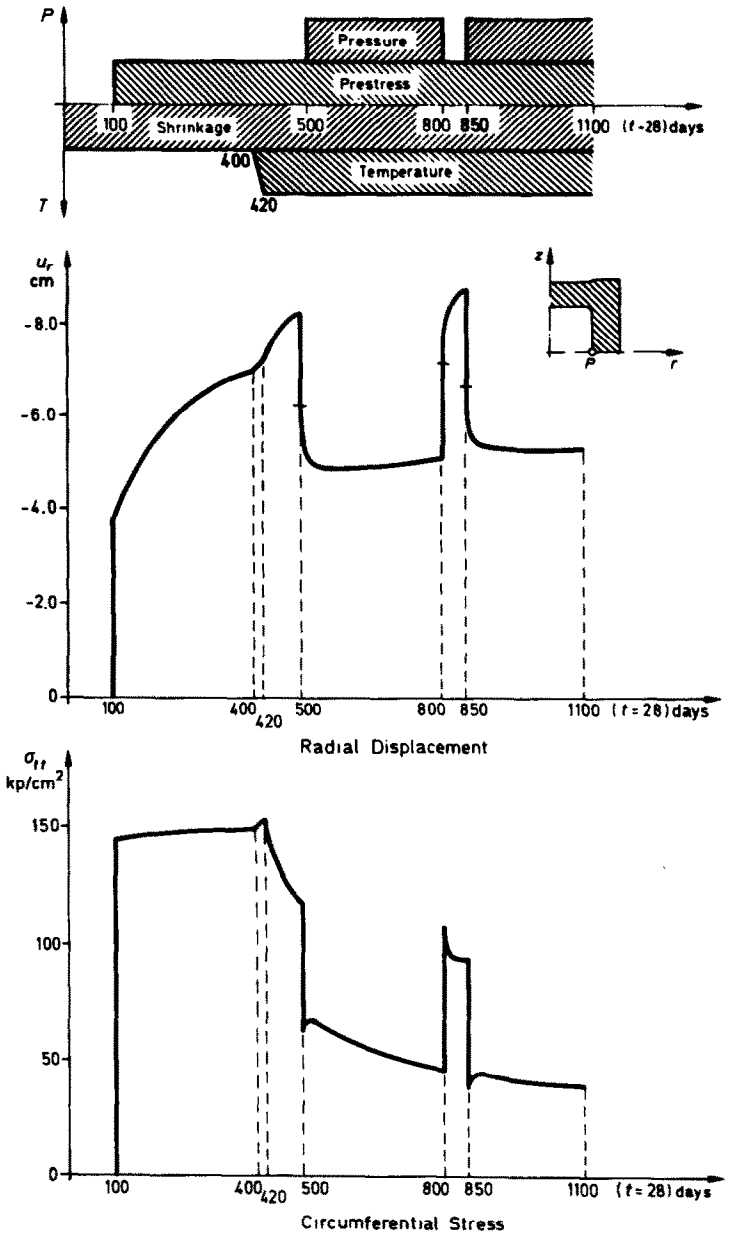

Fig. 5.10. Response history at point P, with shrinkage.

on the inside surface is also exposed to shrinkage, which relaxes the stress level on the inside wall by approximately 50 kp/cm² and redistributes the peak values towards the interior of the containment wall.

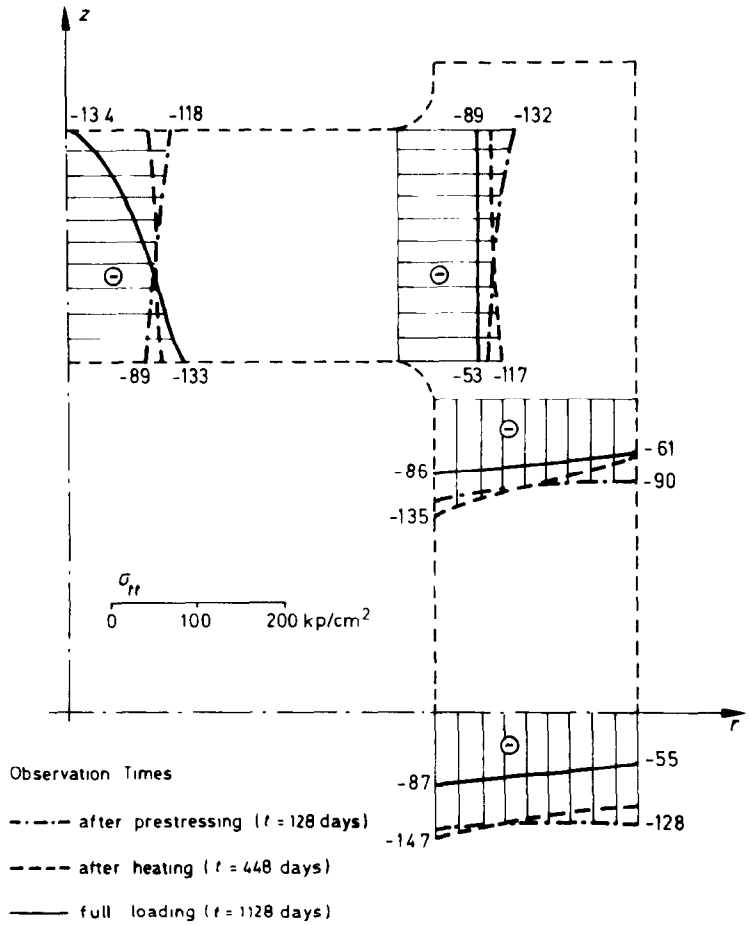

Fig. 5.11. Circumferential stress distribution, no shrinkage.

6. Concluding remarks

The objective of the paper was to develop a unified constitutive model for the numerical solution of concrete creep problems. Particular attention was given to models suitable for computer-oriented solution of complex engineering structures with realistic loading histories involving temperature and humidity in addition to mechanical effects such as prestress and cycling pressure.

The structure of the proposed creep law is sufficiently general to accommodate aging and hereditary effects, which are reflected by the evolution of internal variables controlling the creep process. Parameter identification from test data was examined for five different creep models which correspond to creep analysis methods appearing in the concrete literature. Using an objective least squares procedure, the summation model provides the same accuracy as product and time shift strategies for the data of Browne and Bamforth [24]. An incremental numerical algorithm incorporating variable time steps and retaining history effects without explicit storage of previous results was developed. After extension to multiaxial stress conditions, constitutive equations were projected

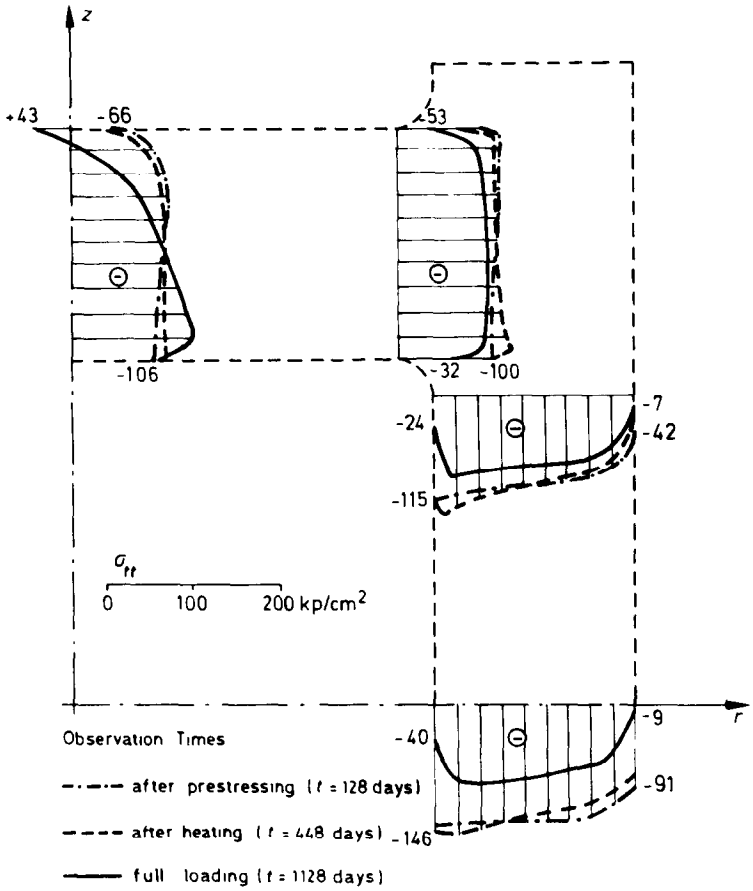

Fig. 5.12. Circumferential stress distribution, with shrinkage.

onto the structural level by the finite element, initial load method. For illustration, the computer-oriented creep analysis method was applied to a complex engineering problem, a prestressed concrete reactor vessel subjected to a realistic loading history.

Finally, we note that the proposed creep model has sufficient flexibility to describe qualitatively all predominant creep phenomena in concrete, provided that strain depends linearly on stress history. Extension to the nonlinear range is possible, but the structure of the constitutive equations is no longer unique. At the present time available creep data of the Wylfa concrete do not suffice to identify the model parameters as functions of humidity and transient environments, where additional effects such as transitional thermal creep and drying creep have been observed.

Acknowledgement

The authors would like to thank Ernst Peter Warnke for his contributions to the thermodiffusion analysis.

This study was supported by the Ministry of Research and Technology, Federal Republic of Germany, grant SBB 4, under the guidance of Dr. N. Bunke whose help is gratefully acknowledged.

Appendix. Summation model for Wylfa concrete

The creep strain increment $\Delta_j\gamma$ in the time step Δt_j is made up of five components

$$\Delta_j\gamma = \Delta_j\epsilon + \Delta_j\eta_F + \Delta_j\eta_D + \Delta_j\eta_T + \Delta_j\eta_H \ , \tag{4.2}$$

whose parameters are summarized below for the Wylfa concrete [24, 25].

1. Elastic component: $\Delta_j\sigma = E(t_j, T_j)\Delta_j\epsilon$ (4.8)

Time and temperature dependence of the elastic compliance are shown in fig. 5.6 for the parameters of (3.10) with

$$E(t_j, T_j) = \sum_{i=1}^{6} \{a_i(T_{20}) + [a_i(T_{95}) - a_i(T_{20})]\,\bar{T}_j\} \exp(-c_i t_j) \ , \qquad \bar{T}_j = (T_j - 20)/75 \ , \tag{A.1}$$

and

i	c_i	$a_i(T_{20})$	$a_i(T_{95}) - a_i(T_{20})$
1	0	0.113	31.168
2	0.3	64.791	−64.791
3	0.03	0.819	10.280
4	0.003	0	1.092
5	0.0003	10.766	−10.687
6	0.00003	25.248	−13.271

(A.2)

2. Flow component: $\Delta_j\eta_F = A_1^2\,\sigma(t_j)\Psi[t_j, T_j]\,\Delta_j t$ (4.11)

Time and temperature dependence of the flow compliance are shown in fig. 5.7 for the parameters of eq. (3.51)

$$A_1^2 = 0.025 \ , \qquad \Psi(t_j, T_j) = t_j^{-0.975}(471 - 471\bar{T}_j), \qquad \bar{T}_j = (T_j - 20)/75 \ . \tag{A.3}$$

3. Delayed component: $\Delta_j\eta_D = \sum_{\alpha=2}^{6} [\mu(t_j, T_j) + \Delta\mu(t_j, T_j)]_\alpha$ (4.13)

Time and temperature dependence of the delayed elastic compliance are shown in fig. 5.8 for the parameters of eq. (3.53). The single step recursion formula (4.14) expresses μ_j in terms of μ_{j-1} and the increment $\Delta_{j-1}\mu$ according to eq. (4.17) for non-aging behaviour:

$$\Delta\mu(t_j, T_j)_\alpha = \frac{\mathcal{J}_\alpha^*(T_j)\sigma(t_j^*)}{\lambda_\alpha}\,[1 - \exp(-\lambda_\alpha \Delta_j t)] \tag{A.4}$$

and

$$\mathcal{J}_\alpha^*(T_j) = \mathcal{J}_\alpha(T_{20}) + [\mathcal{J}_\alpha(T_{95}) - \mathcal{J}_\alpha(T_{20})]\,\bar{T}_j \ , \qquad \bar{T}_j = (T_j - 20)/75 \ .$$

From (3.34) and (3.47) the governing parameters λ_α and $\mathcal{J}_\alpha$ are

i	λ_α	$\mathcal{J}_\alpha(T_{20})$	$\mathcal{J}_\alpha(T_{95}) - \mathcal{J}_\alpha(T_{20})$
1	3.0	11.7	22.8
2	0.3	0.865	7.265
3	0.03	0.0	0.672
4	0.003	0.019	0.048
5	0.0003	0.0018	0.0055

(A.5)

4. Thermal component: $\Delta_j \eta_T = \alpha(t_j, T_j)\, \Delta_j T$ (4.18)

For this particular concrete with calcitic aggregate a constant coefficient of instantaneous thermal expansion is used:

$$\alpha(t_j, T_j) = 6 \times 10^{-6} = \text{const.} \tag{A.6}$$

5. Hygral component: $\Delta_j \eta_H = \beta(t_j, H_j)\, \Delta_j T$ (4.20)

The moisture dependence of the coefficient of instantaneous hygral expansion is shown in fig. 5.4 as proposed in [38]:

$$\beta(t_j, H_j) = \beta_0 (1 - 0.95H^3 - 0.25H^{20}), \quad \beta_0 = 7 \times 10^{-4}, \quad 0 \leqslant H \leqslant 1. \tag{A.7}$$

References

[1] D. Mc Henry, A new aspect of creep in concrete and its application in design, ASTM 43 (1943) 1069–1084.
[2] N.Ch. Arutyunyan, Some problems in the theory of creep (Pergamon Press, 1966).
[3] A.D. Ross, Creep of concrete under variable stress, J. ACI 29 (1958) 739–758.
[4] H. Trost, Auswirkungen des Superpositionsprinzips auf Kriech- und Relaxationsprobleme bei Beton und Spannbeton. Beton und Stahlbetonbau 62 (1967) 232–238 and 65 (1970) 155–179.
[5] A.H. Neville and W. Dilger, Creep of concrete: plain, reinforced and prestressed (North Holland, Amsterdam, 1970).
[6] Z. Bazant, Creep and Shrinkage of concrete: a precis of recent developments, Mechanics Today 2, Nemat-Nasser (ed.), Pergamon Press (1974) 1–93.
[7] J.L. Sackman, Creep in concrete and concrete structures, Proceedings Princeton Univ. Conference on Solid Mechanics, Princeton, N.J. (1963) 15–48.
[8] J.M. Illston and P.D. Sanders, Characteristics and prediction of creep of a saturated mortar under variable temperature, Mag. Concrete Res. 26 (1974) 169–179.
[9] Z.P. Bazant and S.T. Wu, Creep and shrinkage law for concrete at variable hunidity, ASCE, Eng. Mech. J. EM 6 (1974) 1183–1209.
[10] Z.P. Bazant and S.T. Wu, Thermoviscoelasticity of aging concrete, ASCE, J. Eng. Mech. Div. EM 3, 100 (1974) 575–597.
[11] B.R. Gamble and I.J. Jordaan, A direct method of viscoelastic analysis for aging concrete, Mat. Struc,, RILEM 7 (1974) 37–43.
[12] H. Rüsch, D. Jungwirth and H. Hilsdorf, Kritische Sichtung der Verfahren zur Berücksichtigung der Einflüsse von Kriechen und Schwinden des Betons auf das Verhalten der Tragwerke, Beton und Stahlbetonbau 68 (1973) 49–60, 76–86, 152–158.
[13] J.H. Argyris, K.S. Pister and K.J. Willam, Thermomechanical creep of aging concrete, a unified approach, IABSE Publ. 36–1 (1976) 23–57.
[14] R.A. Schapery, On a thermodynamic constitutive theory and its application to various nonlinear materials, Proc. IUTAM Symposium, East Kilbride (Springer, 1968) 259–285.
[15] K.C. Valanis, A unified theory of thermomechanical behaviour of viscoelastic materials, in mechanical behaviour of materials under dynamic loads, U.S. Lindholm (ed.) (Springer , New York, 1968) 343–364.

[16] P. Perzyna, Internal variable description of plasticity, in: Problems of plasticity, A. Sawczuk (ed.) (Noordhoff, 1974) 145–170.
[17] J. Lubliner, On the structure of the rate equations of materials with internal variables, Acta Mech. 17 (1973) 109–119.
[18] H. Dettling, Die Wärmedehnung des Zementsteines, der Gesteine und der Betone, Rep. No. 3 (Otto Graf Inst., Univ. Stuttgart, 1962).
[19] F. Dischinger, Untersuchungen über die Knicksicherheit, die elastische Verformung und das Kriechen des Betons bei Bogenbrücken, Bauingenieur 18 (1937) 487–520, 539–552, 595–621 and 20 (1939) 53–63, 286–294, 426–437, 563–572.
[20] J.M. Illston, The components of strain in concrete under sustained compressive stress, Mag. Concrete Res. 17 (1965) 21–28.
[21] Z.P. Bazant and S.T. Wu, Dirichlet series creep function of aging concrete ASCE, J. Eng. Mech. Div. EM 2 (1973) 367–387.
[22] M.A. Mukaddam and B. Bresler, Behaviour of concrete under variable temperature and loading, ACI Spec. Publ. no. 34, ACI Seminar on Concrete in Nuclear Reactors, Berlin (1970) 771–797.
[23] Y.R. Rashid, Nonlinear analysis of two-dimensional problems in concrete creep, ASME, J. Appl. Mech. 39 (1972) 475–482.
[24] R.D. Browne and P.B. Bamforth, The long term creep of the Wylfa P.V. concrete for loading ages up to 12.5 Years, Paper H 1/8, 3rd SMIRT Conference, London (Sept. 1–5, 1975).
[25] R.D. Browne and R. Blundell, The influence of loading age and temperature on the long term creep behaviour of concrete in a Sealed moisture stable State, Materials and Structures, RILEM 2 (1969) 133–144.
[26] U. Schneider and K. Kordina, On the behaviour of normal concrete under steady state and transient temperature conditions, Paper H 1/6, 3rd SMIRT Conference, London (Sept. 1–5, 1975).
[27] K.S. Pister, Some thoughts on the material identification problem, Workshop on Appl. Thermoviscoplasticity, Northwestern Uni., Evanston, Ill. (Oct., 13–14, 1975).
[28] Z.P. Bazant and E.M. Osman, On the choice of creep function fo standard recommendations on practical analysis of structures, Cement and Concrete Res. 5 (1975) 129–138.
[29] C. Lanczos, Applied analysis (Prentice Hall, 1956).
[30] K.S. Pister, Constitutive modelling and numerical solution of field problems, Nucl. Eng. Design 28 (1974) 137–146.
[31] H.G. Geymayer, Effect of temperature on creep on concrete, A literature review, ACI SP-34, 1 (1972) 565–590.
[32] J.M. Illston and I.J. Jordaan, Creep prediction for concrete under multiaxial stress, ACI J. 69–14 (1972) 158–164.
[33] J.H. Argyris, K.E. Buck, D.W. Scharpf and K.J. Willam, Nonlinear methods of structural analysis, Nucl. Eng. Design 19 (1972) 169–197.
[34] J.H. Argyris, G. Faust, J.R. Roy, J. Szimmat, E.P. Warnke and K.J. Willam, Finite Elemente zur Berechnung von Spannbeton-Reaktordruckbehältern, DAfStb Proc. 234 (1973).
[35] J.H. Argyris, G. Faust, J. Szimmat, E.P. Warnke and K.J. Willam, SMART-Strukturmechanische Analyse in der Reaktortechnologie, DAfStb Proc., SBB-Seminar, No. 2/1, Berlin (Oct. 13–14, 1975).
[36] J. Szimmat and K.J. Willam, Parameterberechnungen an einem Referenzbehälter, DAfStb Proc. 237 (1974) 53–66.
[37] J. Hundt, Wärme- und Feuchtigkeitsleitung in Beton under Einwirkung eines Temperaturgefälles, DAfStb Proc. 256 (1975).
[38] Z.P. Bazant and L.J. Najjar, Drying of concrete as a nonlinear diffusion Problem, Cement and Concrete Res. 1 (1971) 461–473.
[39] J.H. Argyris, E.P. Warnke and K.J. Willam, Zur Berechnung von Temperatur und Feuchtefeldern mit finiten Elementen, DAfStb Proc. SBB-Seminar, No. 4/5, Berlin (Oct. 13–14, 1975).